

SUPPORTING INFORMATION

Polymers from sugars and CO₂: ring-opening polymerisation and copolymerisation of cyclic carbonates derived from 2-deoxy-D-ribose

Georgina L. Gregory, Gabriele Kociok-Köhn and Antoine Buchard*

*Department of Chemistry, Centre for Sustainable Chemical Technologies,
University of Bath, Claverton Down, Bath BA2 7AY, UK*

Email: a.buchard@bath.ac.uk

Table of Contents

1. NMR Spectra	2
2. Conversion versus Time for homopolymerisation of 1α	12
3. M_n and Đ versus conversion.....	12
4. Reactivity Ratios	13
5. 1β and TMC copolymerisation kinetics	14
6. SEC Traces	15
7. MALDI-ToF Mass Spectrometry	17
8. TGA-MS	19
9. Selected DSC Traces	19
10. Powder Diffraction.....	21
11. DFT Calculations.....	21
11.1 Initiation Step in the ROP of 1 α , 1 β and TMC	21
11.2 Monomer Ring Strain	25
11.2.1 Thermodynamics of ring-opening with MeOH/ ⁱ PrOH.....	25
11.2.2 Isodesmic reaction with dimethylcarbonate	26
12. Single Crystal X-Ray Structures	28
13. References.....	30

1. NMR Spectra

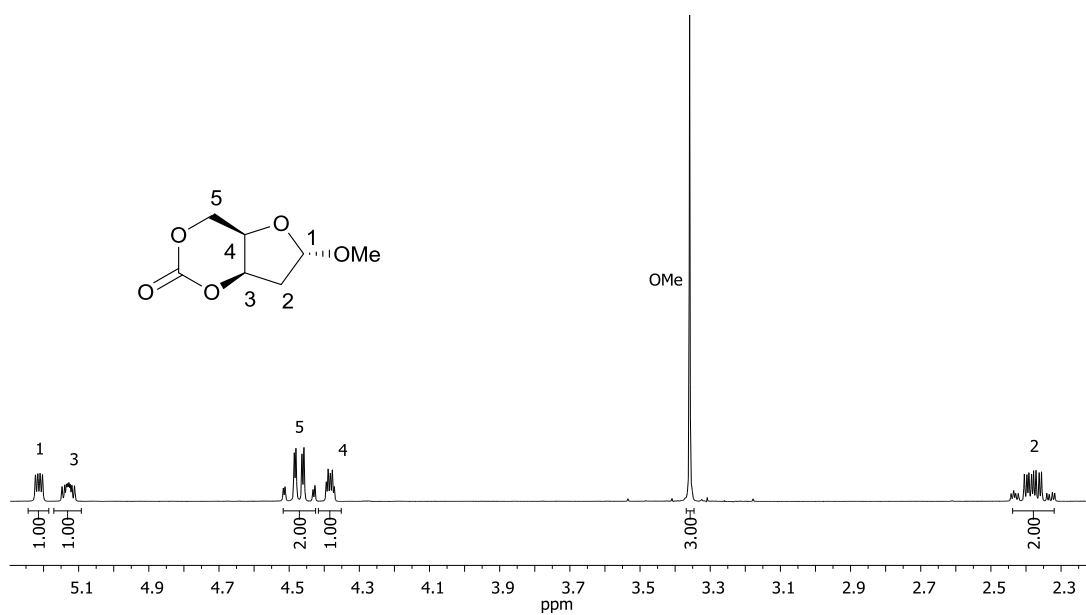


Fig. S1 ¹H NMR spectrum (400 MHz, CDCl₃) of **1α**.

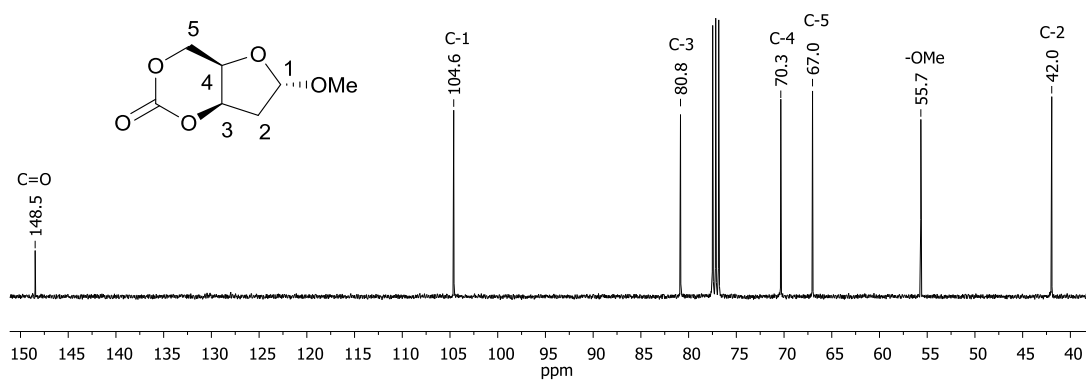


Fig. S2 ¹³C{¹H} NMR spectrum (101 MHz, CDCl₃) of **1α**.

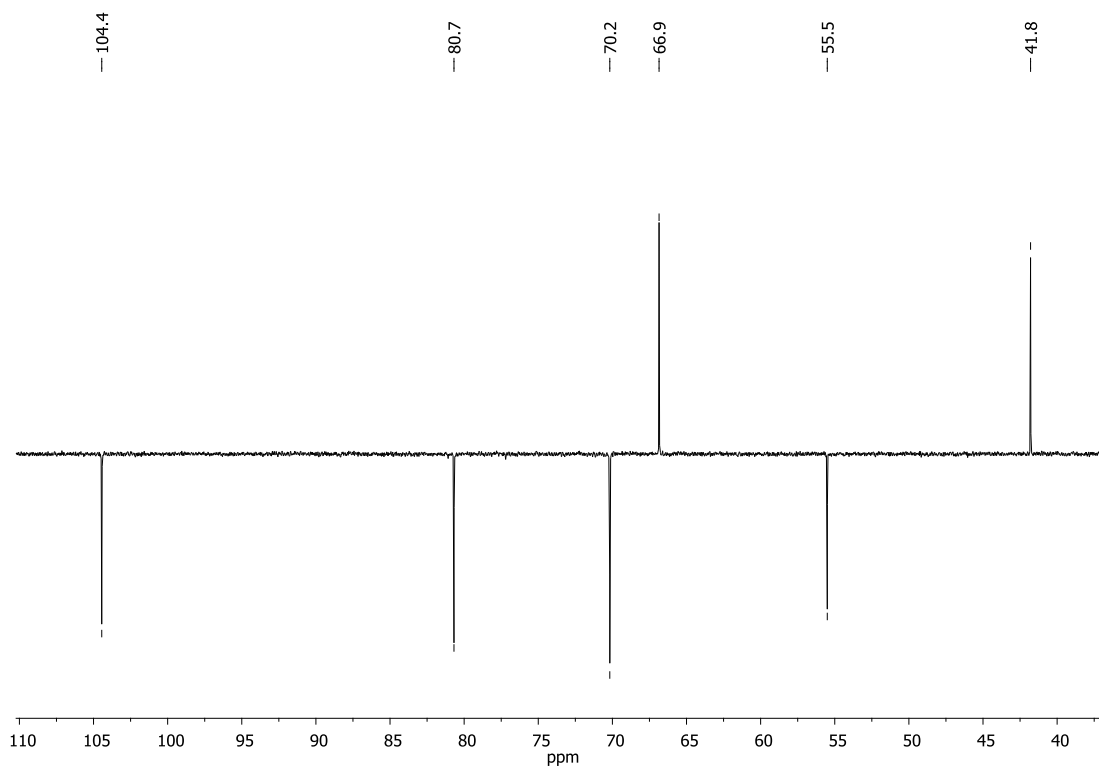


Fig. S3 DEPT135 of **1α** in CDCl_3 .

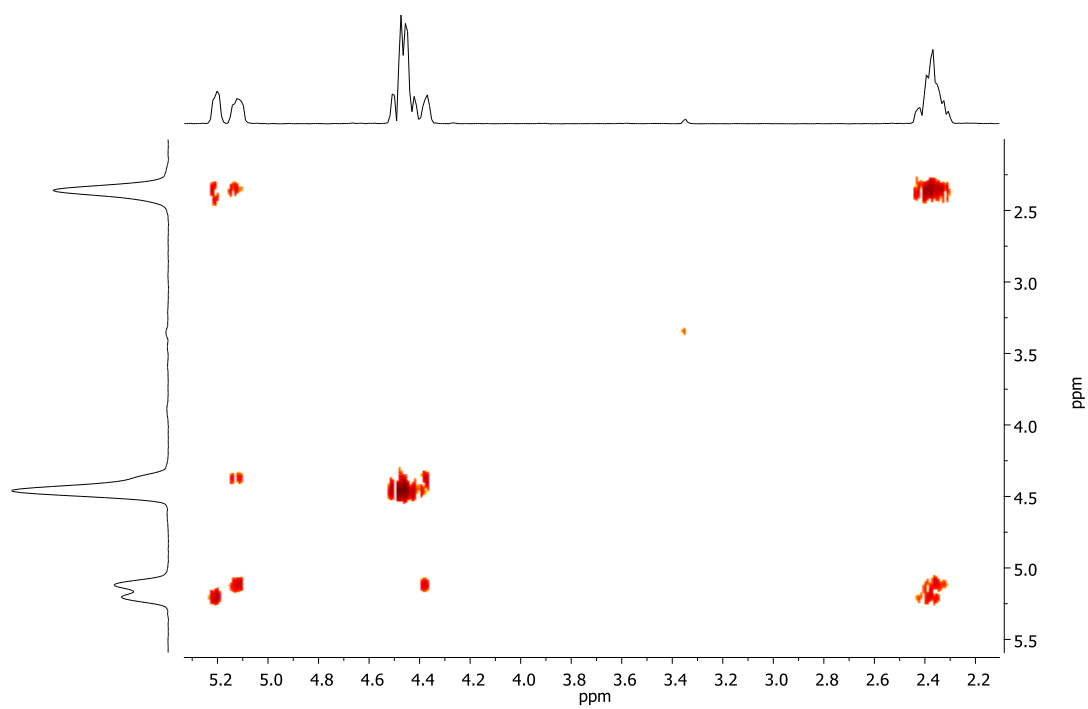


Fig. S4 COSY of **1α** in CDCl_3 .

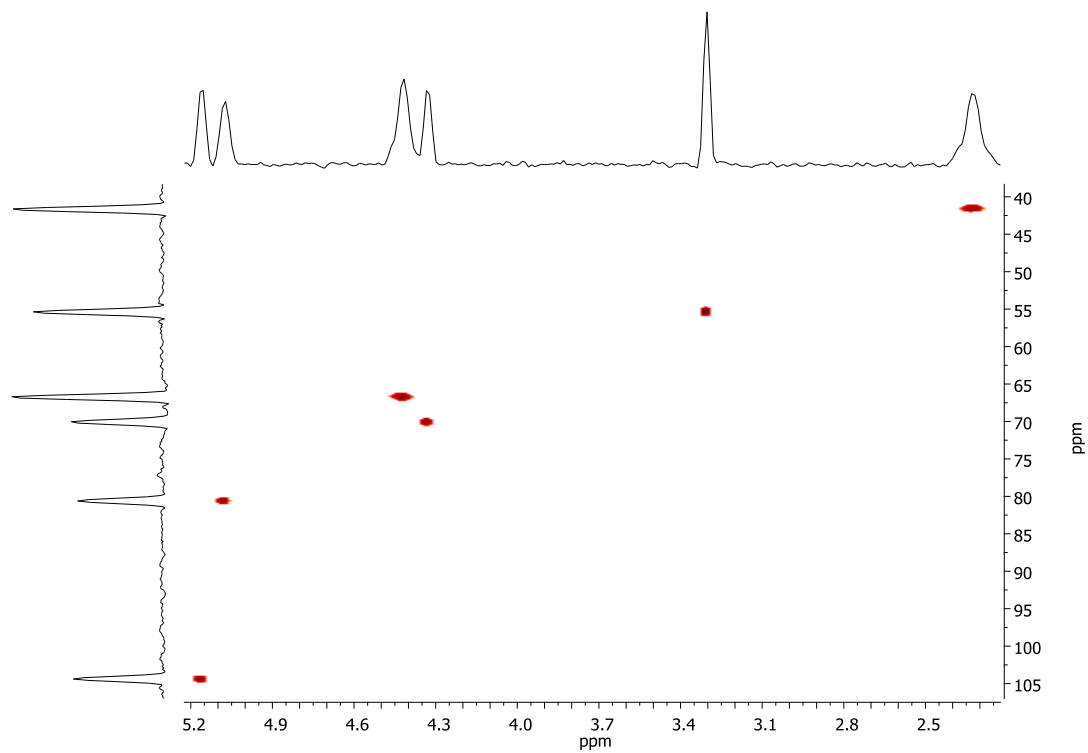


Fig. S5 HSQC of **1α** in CDCl_3 .

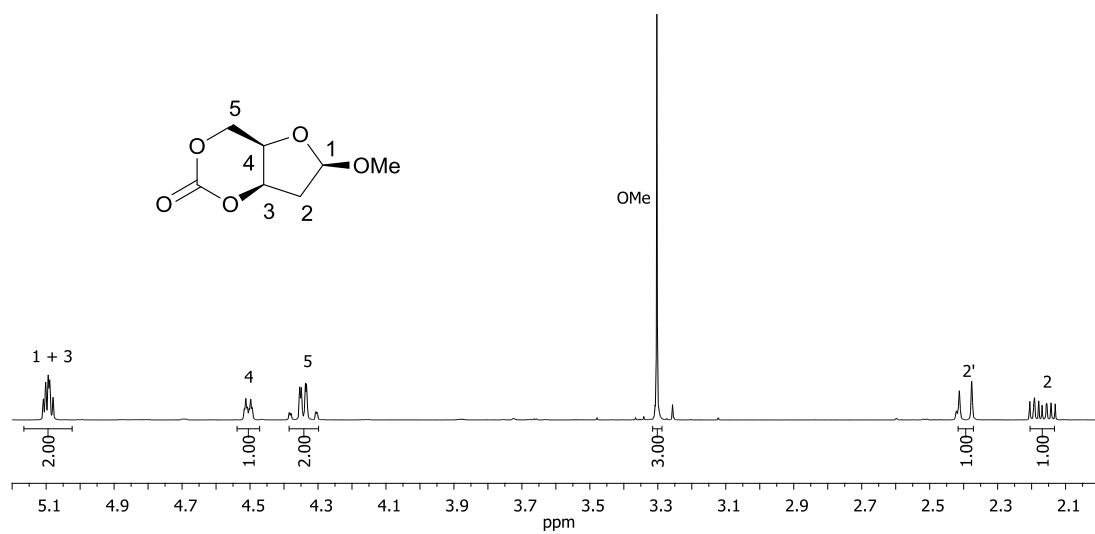


Fig. S6 ^1H NMR spectrum (400 MHz, CDCl_3) of **1β**.

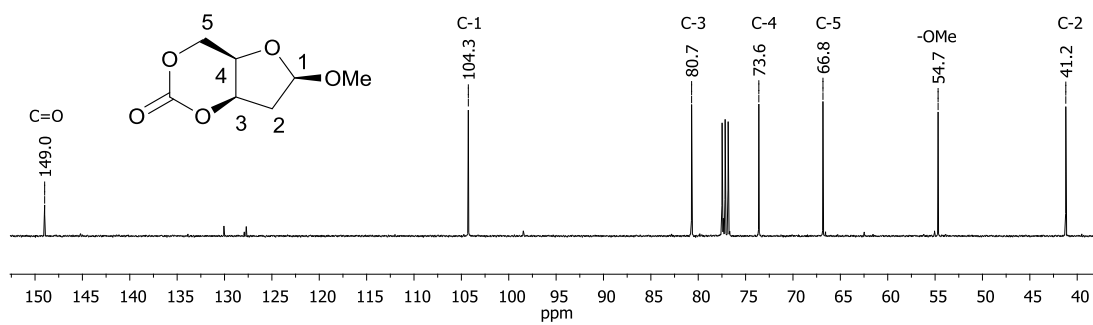


Fig. S7 $^{13}\text{C}\{^1\text{H}\}$ NMR spectrum (101 MHz, CDCl_3) of **1β**.

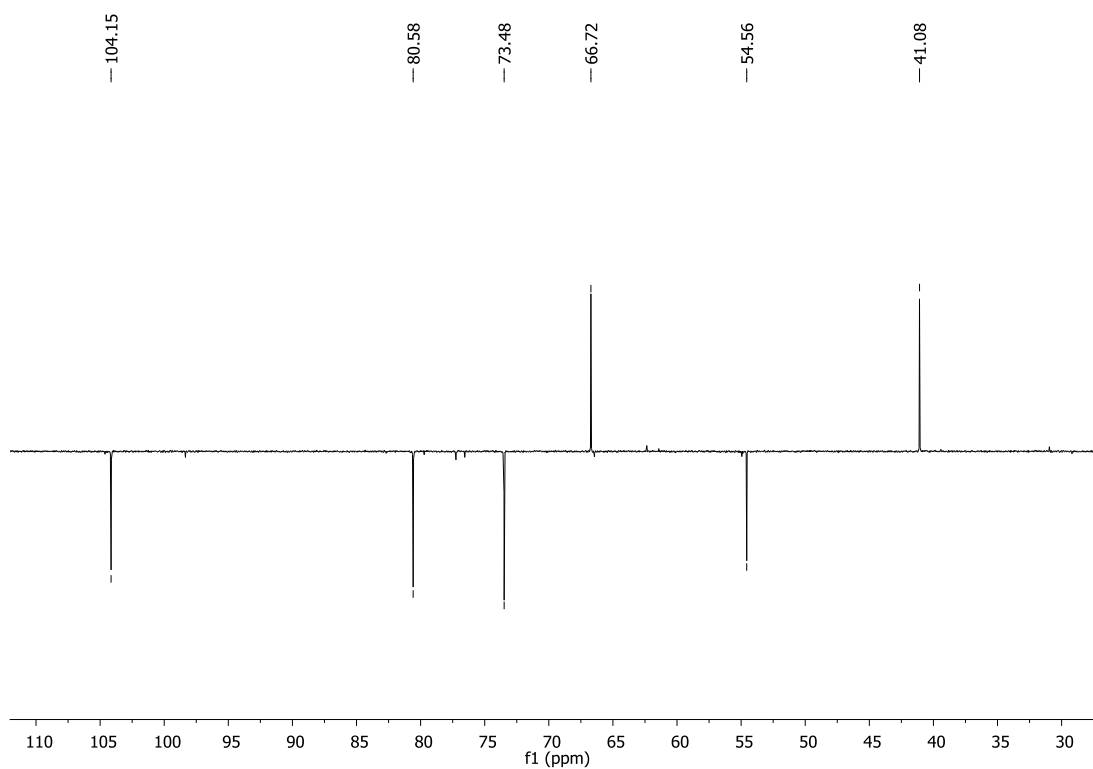


Fig. S8 DEPT135 of **1β** in CDCl_3 .

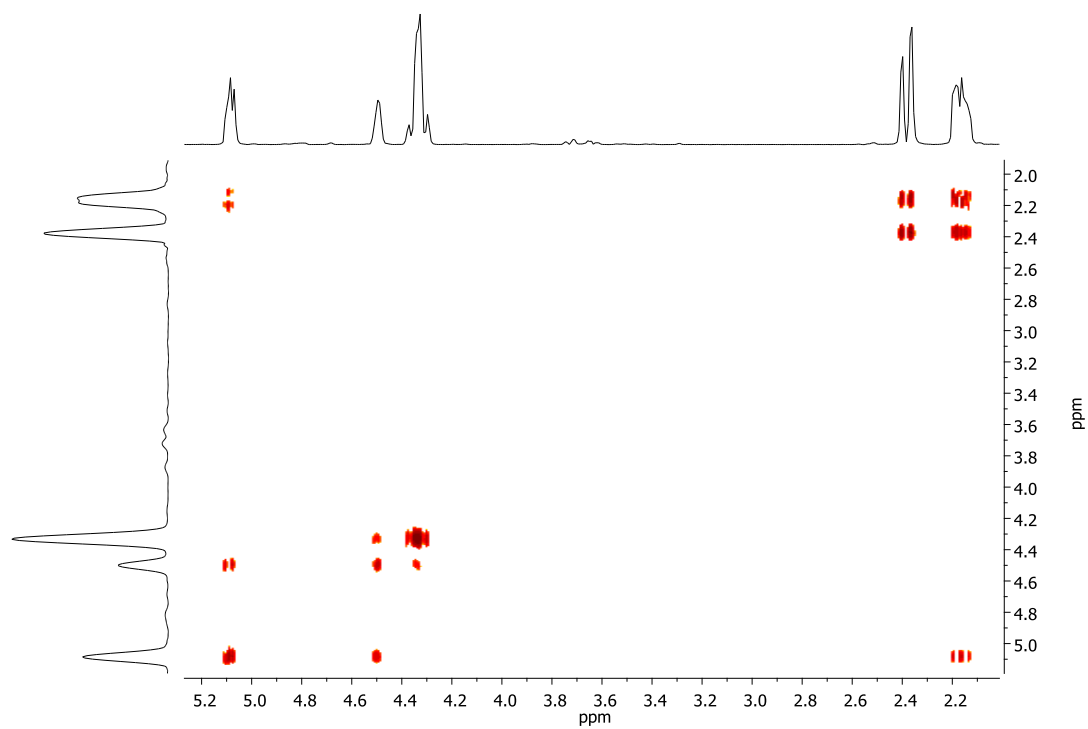


Fig. S9 COSY of **1 β** in CDCl_3 .

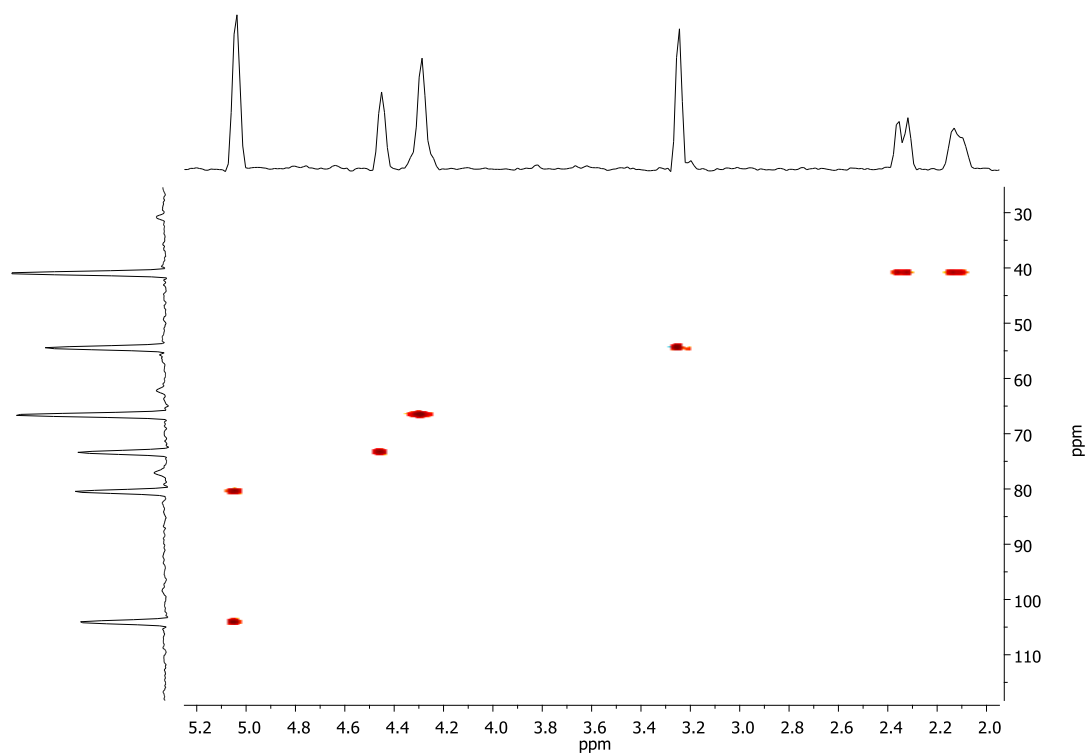


Fig. S10 HSQC of **1 β** in CDCl_3 .

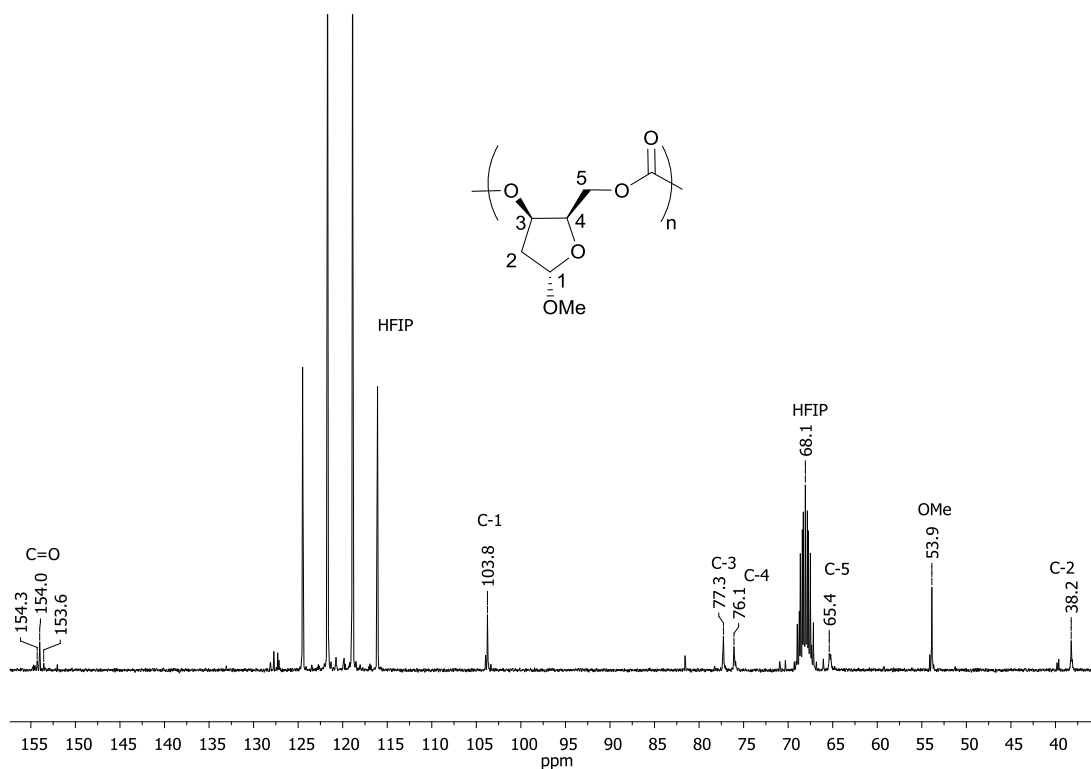


Fig. S11 Complete $^{13}\text{C}\{^1\text{H}\}$ NMR spectrum (400 MHz, HFIP- d_2) of poly(**1a**). Small additional resonances are assigned to unreacted monomer and benzoic acid used to quench the polymerisation.

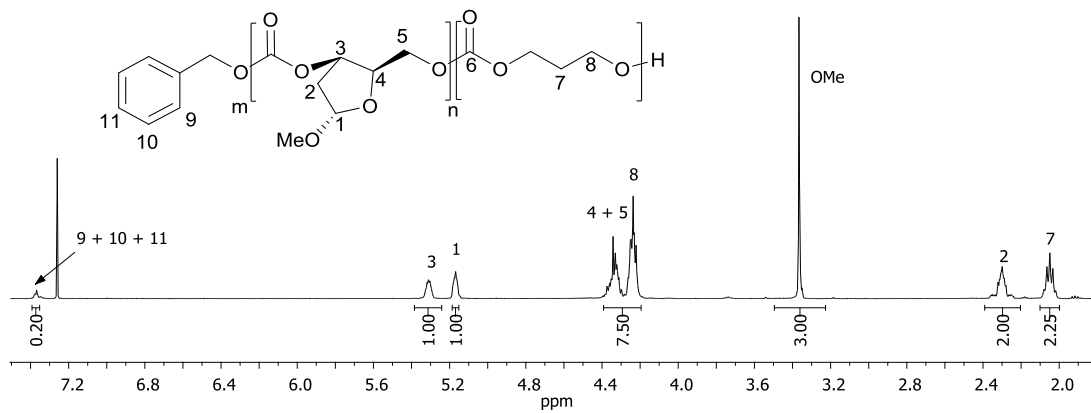


Fig. S12 ^1H NMR spectrum (400 MHz, CDCl_3) of poly(TMC-co-47mol%-**1a**): $M_{n, \text{NMR}} = 7320 \text{ g mol}^{-1}$ (linear polymer: 25 **1a** and 28 TMC repeat units), $M_{n, \text{SEC}} = 6380 \text{ g mol}^{-1}$ (\bar{D} 1.19), $M_{n, \text{calc}} = 6870 \text{ g mol}^{-1}$ (Table 1, Entry 2).

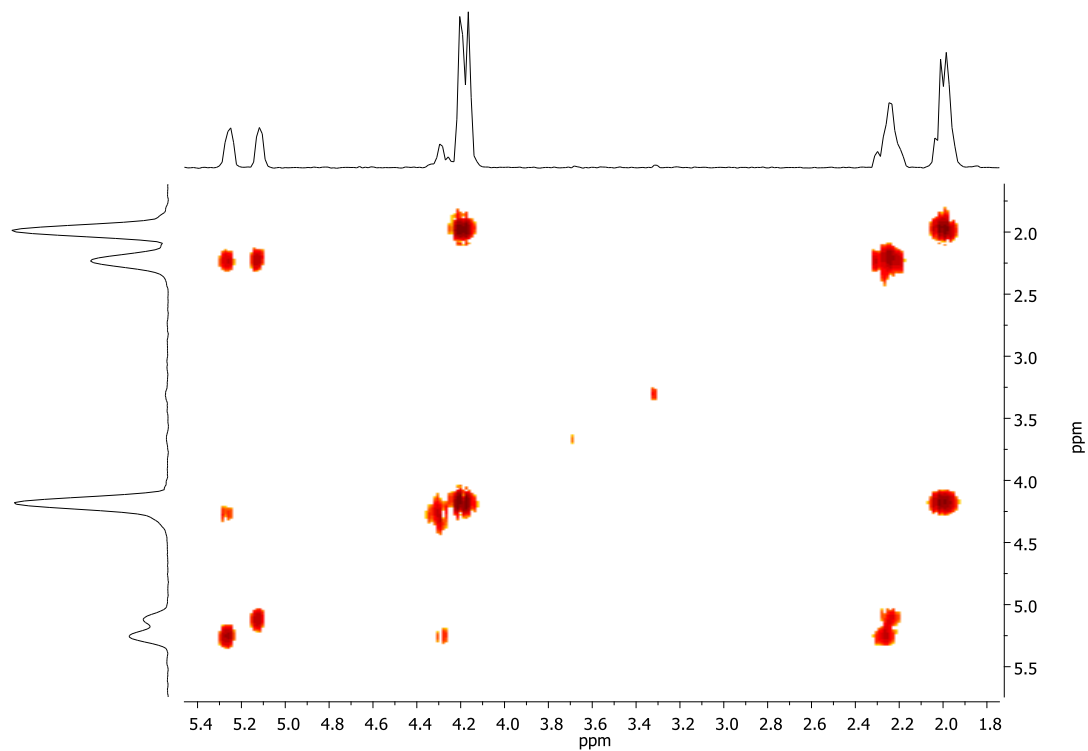


Fig. S13 COSY spectrum (400 MHz, CDCl_3) of poly(TMC-co-47mol%- $\mathbf{1\alpha}$).

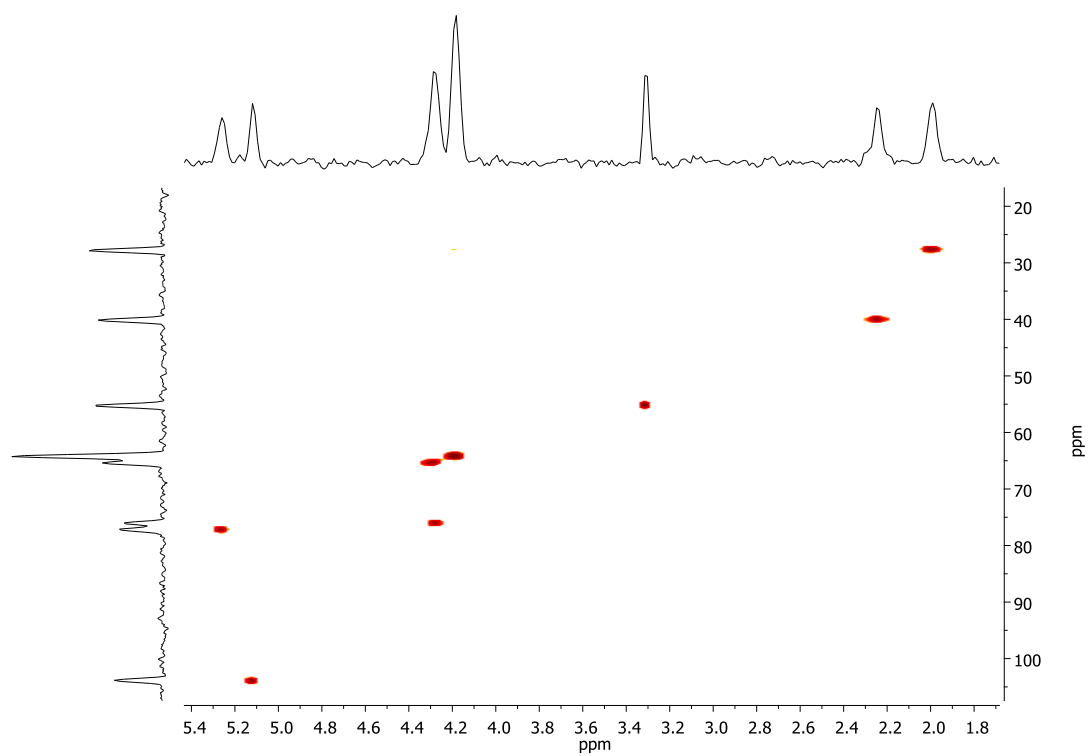


Fig. S14 HSQC of poly(TMC-co-47mol%- $\mathbf{1\alpha}$).

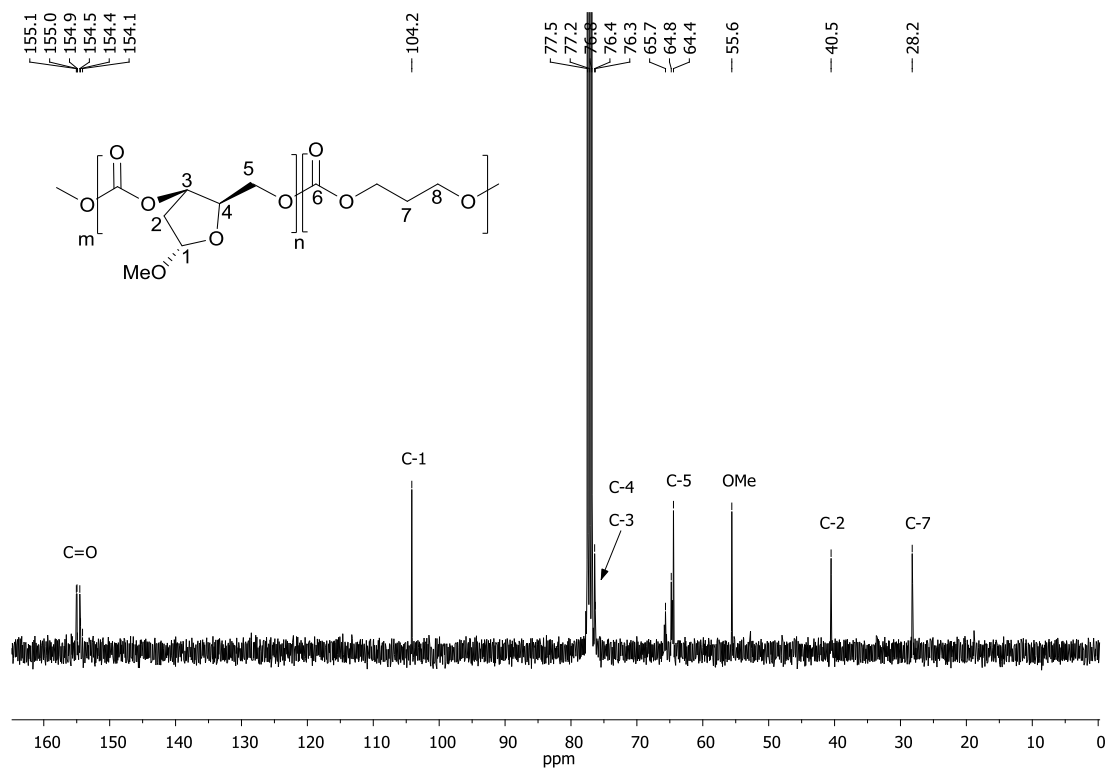


Fig. S15 ¹³C{¹H} NMR spectrum (101 MHz, CDCl₃) of poly(TMC-*co*-47mol%-**1a**).

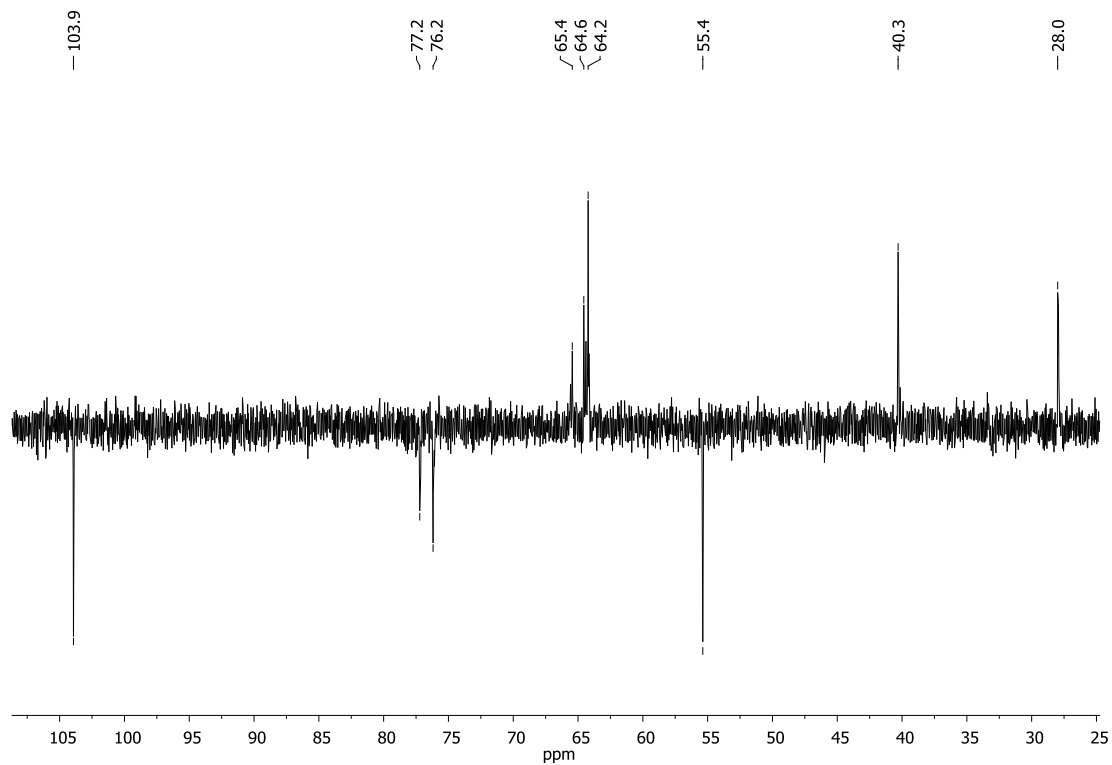


Fig. S16 DEPT135 of poly(TMC-*co*-47mol%-**1a**).

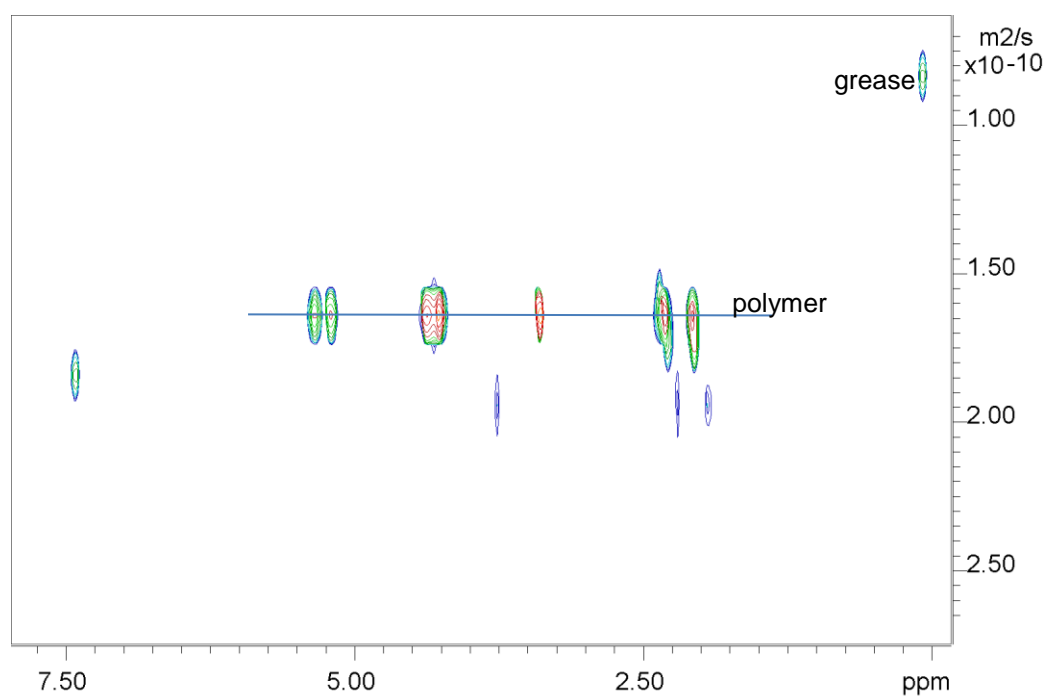
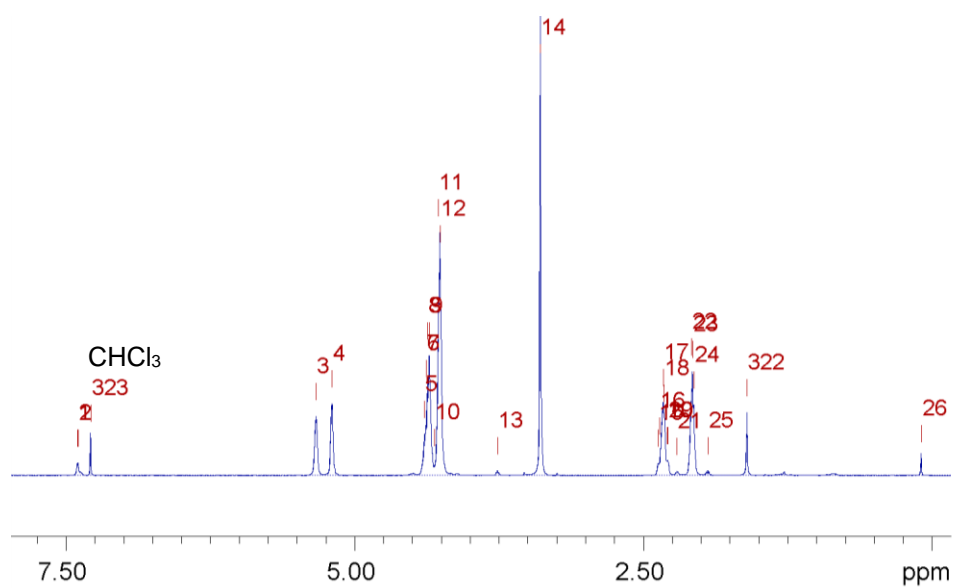


Fig. S17 DOSY Spectra (CDCl₃) of poly(TMC-co-47mol%-1a).

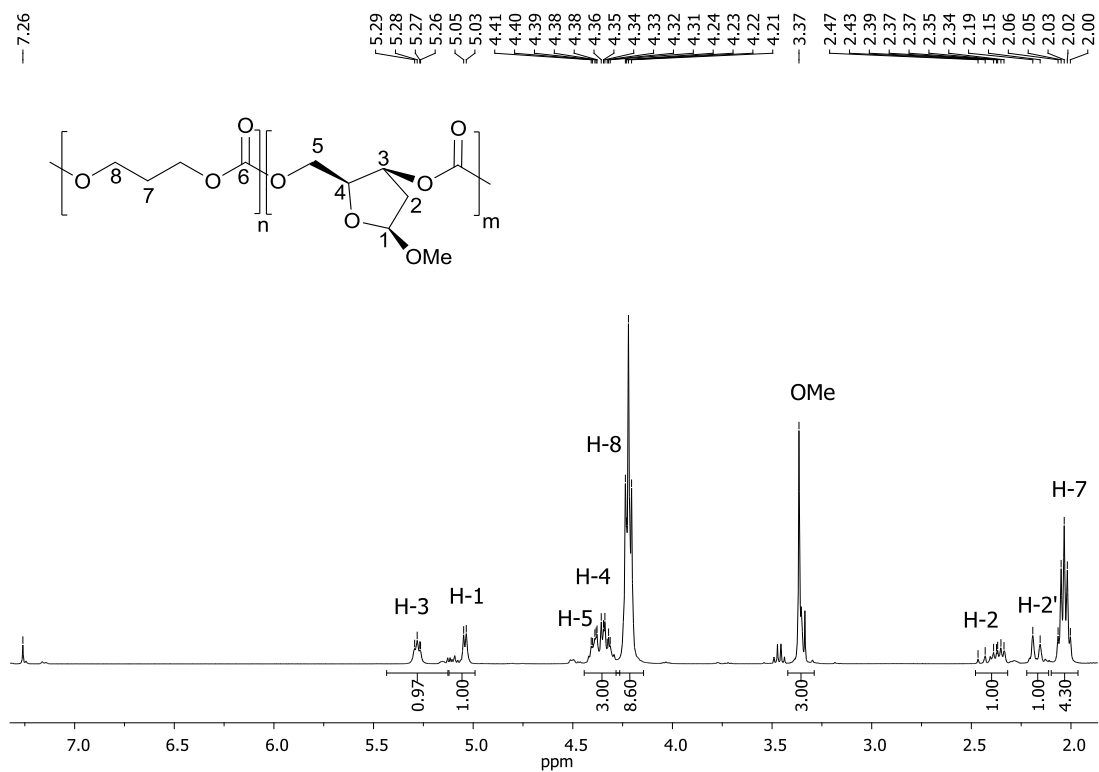


Fig. S18 ¹H NMR spectrum (400 MHz, CDCl₃) of poly(TMC-co-32mol%-1 β): $M_{n, SEC} = 43\ 200\ \text{mol}^{-1}$ ($\bar{D} = 1.39$).

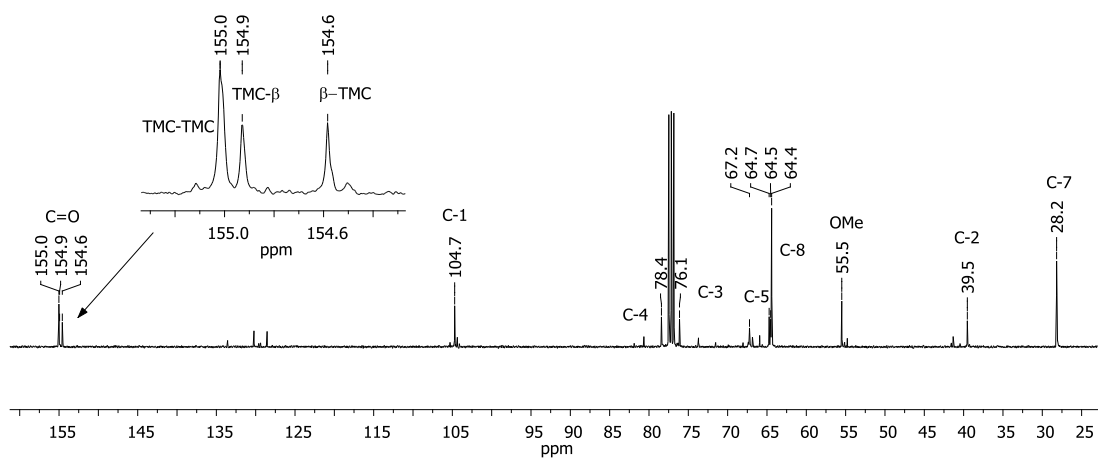


Fig. S19 ¹³C NMR spectrum (101 MHz, CDCl₃) of poly(TMC-co-32mol%-1 β).

2. Conversion versus Time for homopolymerisation of 1 α

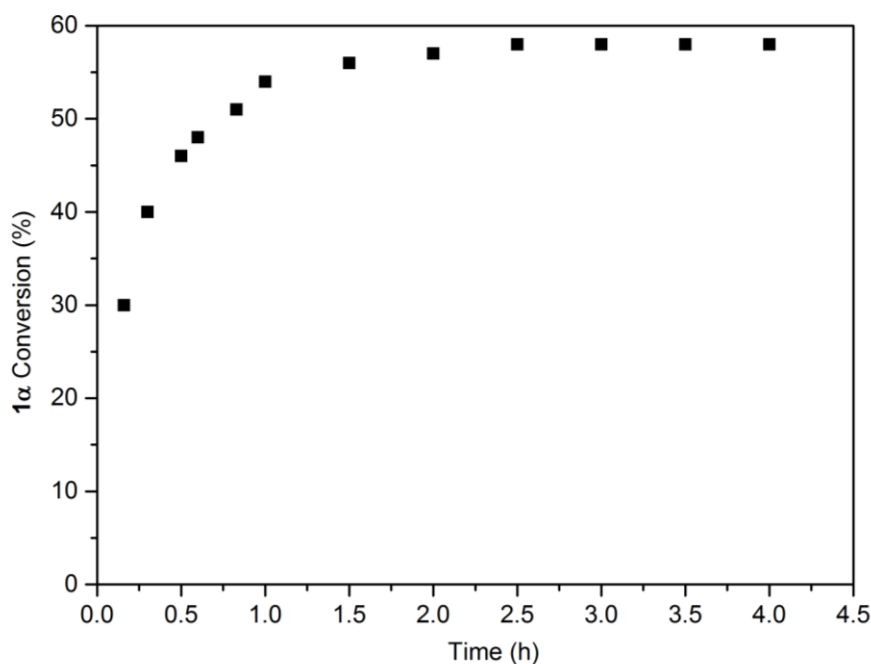


Fig. S20 Conversion of **1 α** as a function of time for a homopolymerisation carried out at rt, $[M]_0 = 5 \text{ mol L}^{-1}$ in CH_2Cl_2 and $[M]_0 : [\text{TBD}]_0 : [\text{BnOH}]_0 = 1000:1:1$. Conversions were determined by ^1H NMR spectroscopy (CDCl_3) from aliquots quenched with benzoic acid.

3. M_n and \bar{D} versus conversion

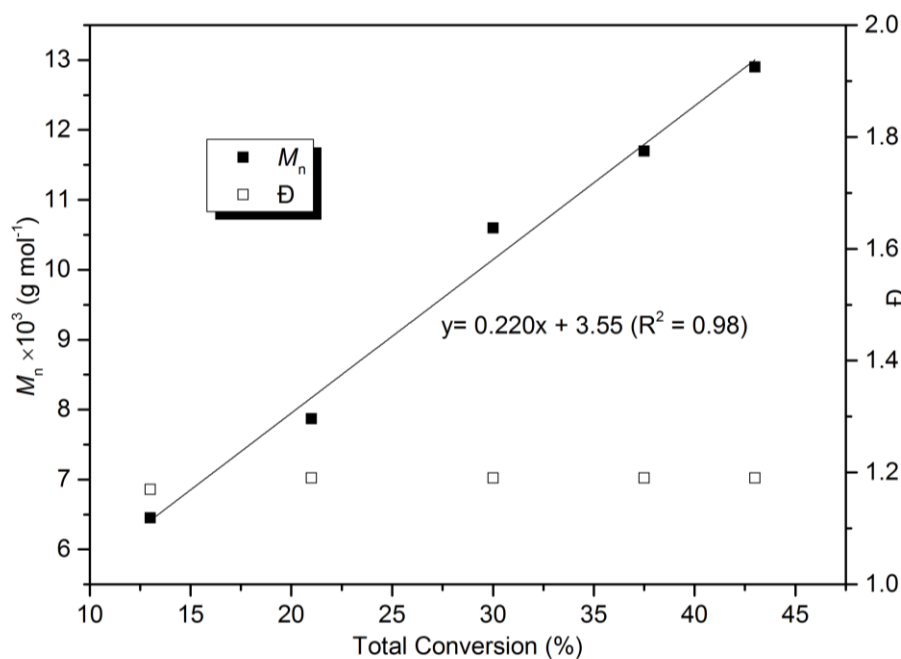


Fig. S21 Linear increase in M_n with monomer conversion whilst maintaining a relatively narrow dispersity ($\bar{D} < 1.2$) for a copolymerisation with **1 α** : TMC feed ratio of 50:50, 1000:1:20 $[M]_0 : [\text{TBD}]_0 : [\text{BnOH}]_0$, $[M]_0 = 5 \text{ mol L}^{-1}$ in CH_2Cl_2 at rt. Monomer conversion was determined by integration of the ^1H NMR spectra of aliquots taken at specific times and quenched with benzoic acid.

acid. For these aliquots, M_n and \bar{D} were estimated by SEC (RI detector) with CHCl_3 eluent versus polystyrene standards.

4. Reactivity Ratios

Polymerisations were carried out at rt with $[\text{M}_t]_0$: $[\text{TBD}]_0$: $[\text{BnOH}]_0$ ratio of 1000:1:1 and $[\text{M}_t]_0 = 5 \text{ mol L}^{-1}$ in CH_2Cl_2 for different feed ratios of **1a** and TMC (f_α and f_{TMC}). Polymerisations were quenched below 15% monomer conversion (<10 minutes) and the copolymer compositions of **1a** and TMC (F_α and F_{TMC}) determined by ^1H NMR spectroscopy.

$$G = H r_{\text{TMC}} - r_\alpha$$

$$G = \frac{f_{\text{TMC}}(2F_{\text{TMC}} - 1)}{(1 - f_{\text{TMC}})F_{\text{TMC}}} \quad H = \frac{f_{\text{TMC}}^2(1 - F_{\text{TMC}})}{(1 - f_{\text{TMC}})^2 F_{\text{TMC}}}$$

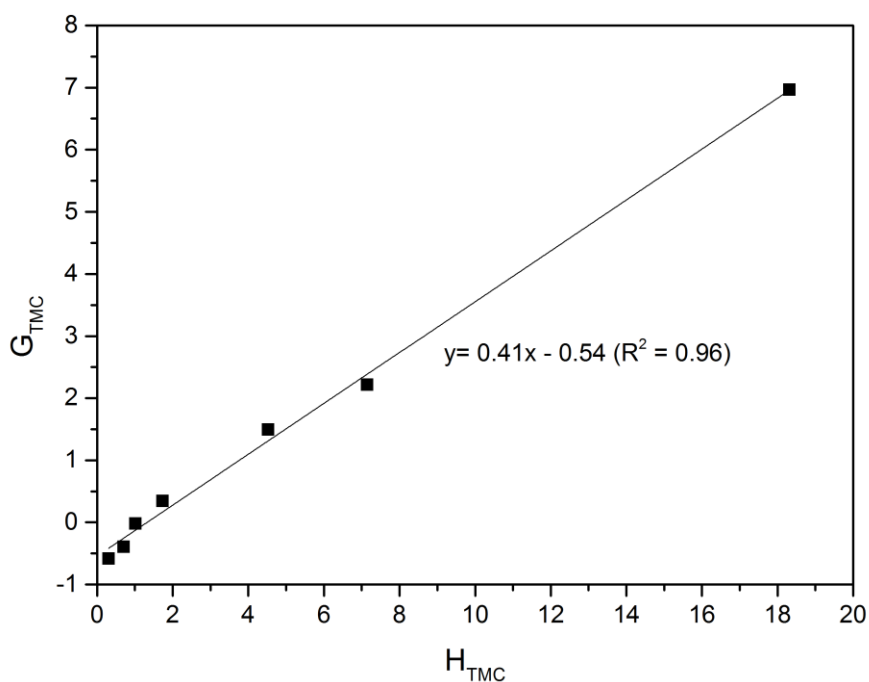


Fig. S22 Calculation of reactivity ratios: r_α and r_{TMC} using the Finemann-Ross method.

5. 1β and TMC copolymerisation kinetics

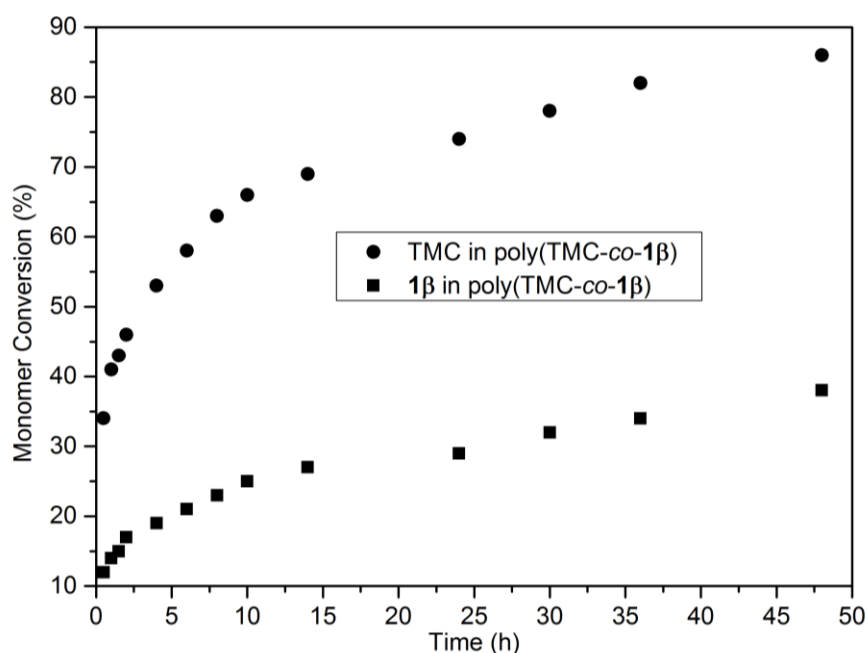


Fig. S23 Monomer Conversion versus time for the copolymerisation of 1β and TMC under the following reaction conditions: $f_{\beta}/f_{\text{TMC}} = 50/50$, $[M]_0 = 5 \text{ mol L}^{-1}$ in CH_2Cl_2 , $[1\beta+\text{TMC}]_0$: $[\text{TBD}]_0$: $[\text{BnOH}]_0$ 1000:1:1, aliquots were taken at specific times, quenched with excess benzoic acid and monomer conversion determined by integration of the ^1H NMR spectra (CDCl_3).

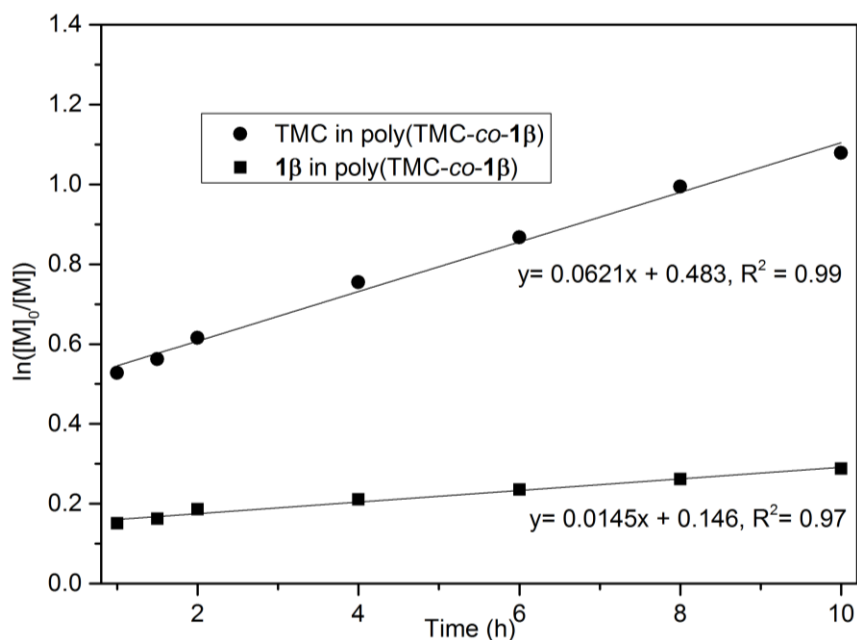


Fig. S24 Kinetic plot for the copolymerisation of 1β and TMC under the following reaction conditions: $f_{\beta}/f_{\text{TMC}} = 50/50$, $[M]_0 = 5 \text{ mol L}^{-1}$ in CH_2Cl_2 , $[1\beta+\text{TMC}]_0$: $[\text{TBD}]_0$: $[\text{BnOH}]_0 = 1000:1:1$, aliquots were taken at specific times, quenched with excess benzoic acid and monomer conversion determined by integration of the ^1H NMR spectra (CDCl_3).

6. SEC Traces

Molecular Weight Averages

Peak	Mp	Mn	Mw	Mz	Mz+1	Mv	PD
Peak 1	67659	63953	84817	110904	139728	106811	1.326

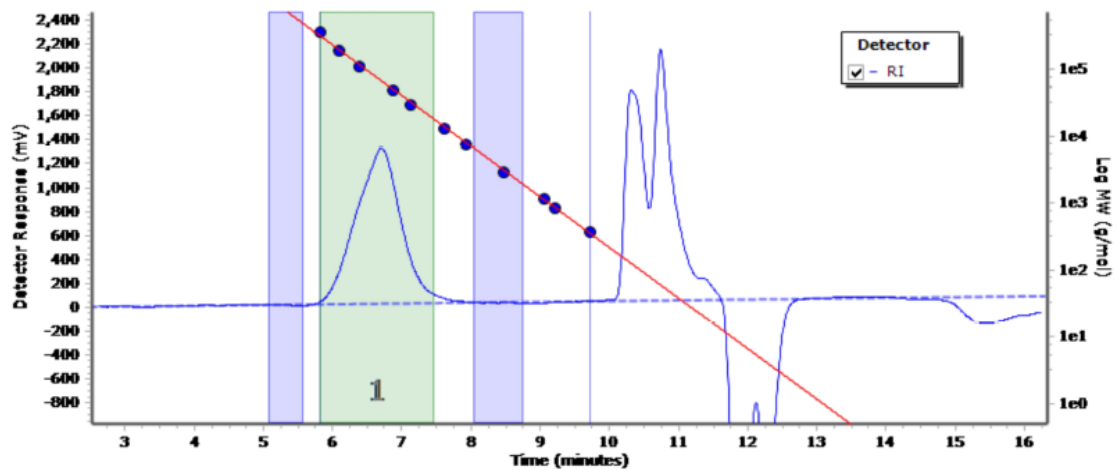


Fig. S25 SEC trace (RI detector *versus* PS standards, CHCl_3 eluent) of poly(TMC-*co*-66mol%-1 α) from Table 1, Entry 1.

Molecular Weight Averages

Peak	Mp	Mn	Mw	Mz	Mz+1	Mv	PD
Peak 1	84804	59136	85349	116542	146691	112011	1.443

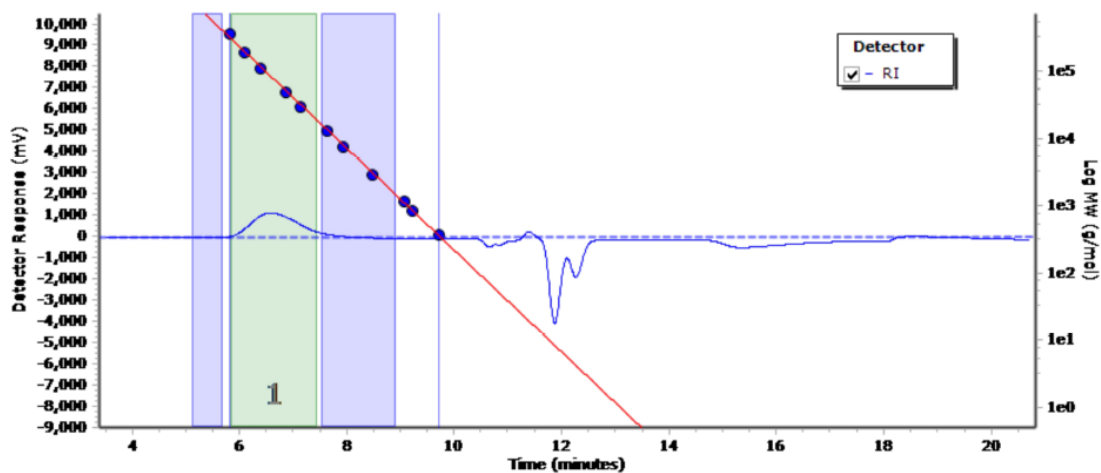


Fig. S26 SEC trace (RI detector *versus* PS standards, CHCl_3 eluent) of poly(TMC-*co*-54mol%-1 α) from Table 1, Entry 4.

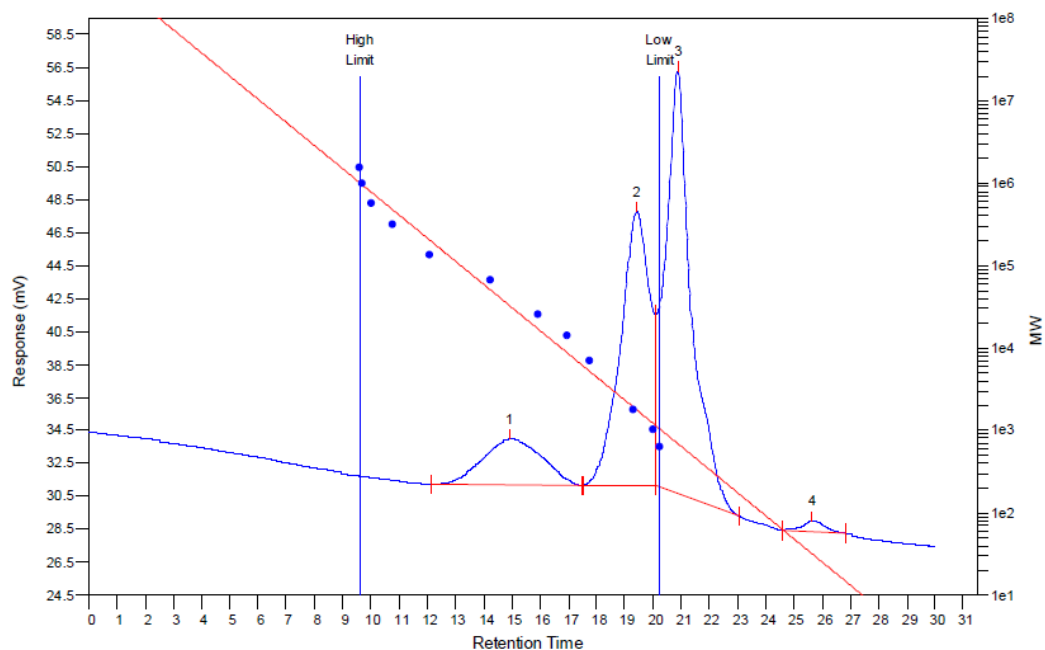


Fig. S27 SEC trace (RI detector *versus* PMMA standards, HFIP eluent) of poly(**1α**) from Table 2, Entry 1. Peak 1 corresponds to an M_n of 25 600 g mol⁻¹ (\bar{D} 1.41) and peak 2 to M_n 1810 g mol⁻¹ (\bar{D} 1.10).

Molecular Weight Averages

Peak	Mp	Mn	Mw	Mz	Mz+1	Mv	PD
Peak 1	51339	43178	59950	79519	97486	76730	1.388

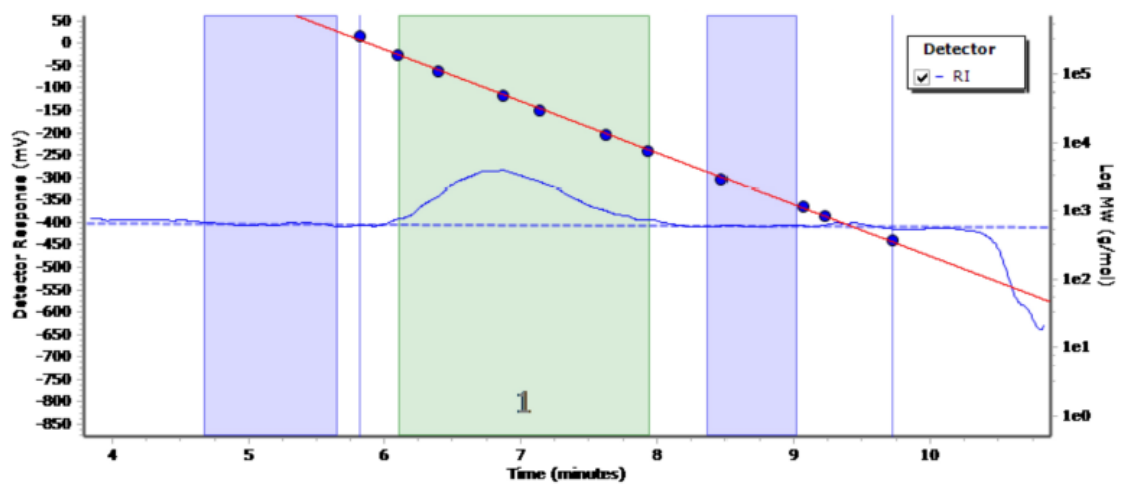


Fig S28 SEC trace (RI detector *versus* PS standards, CHCl₃ eluent) of poly(TMC-co-32mol%-**1β**).

7. MALDI-ToF Mass Spectrometry

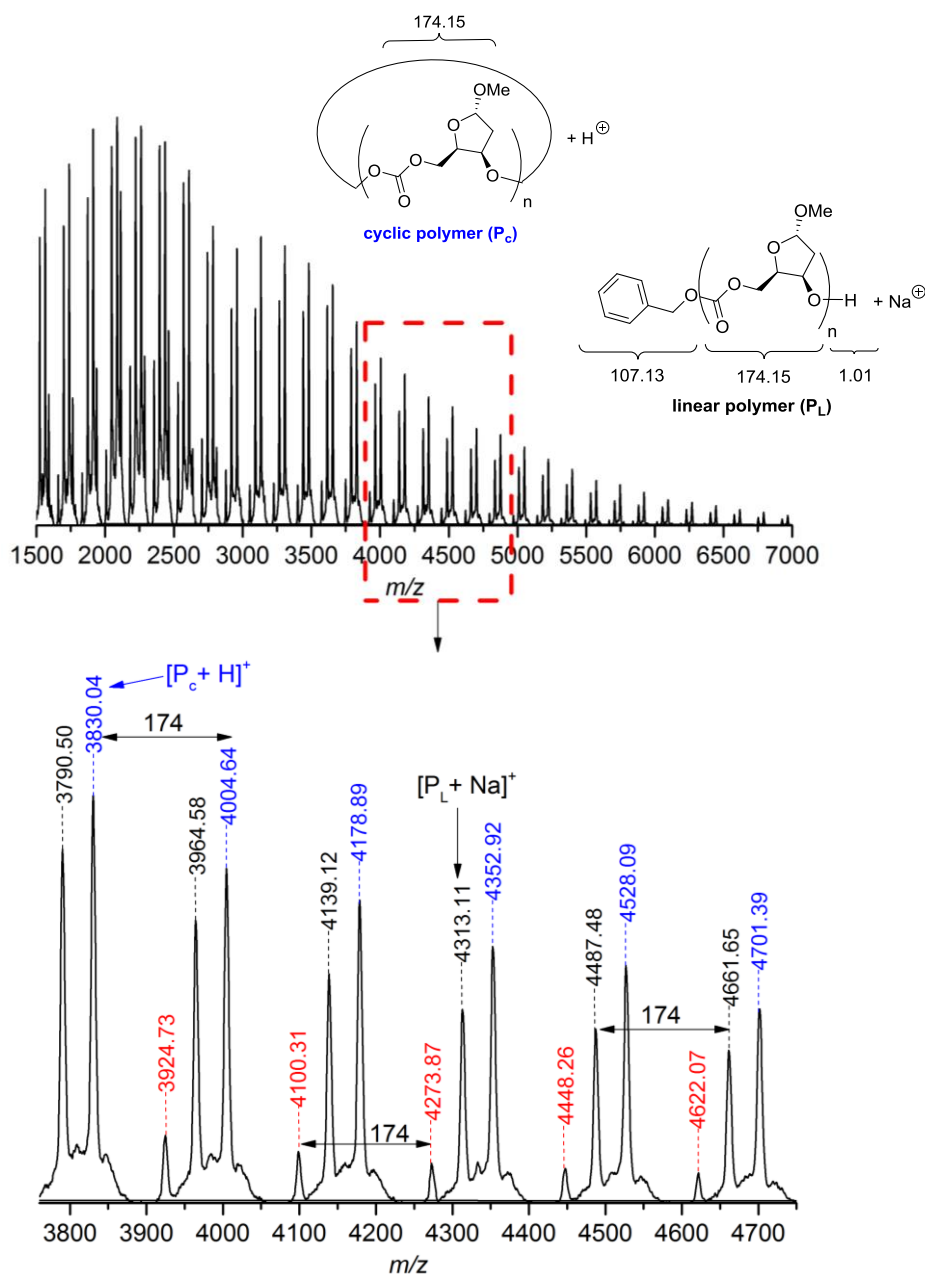


Fig. S29 MALDI-ToF MS of poly(**1a**) showing cyclic polymeric series $[P_c + H]^+$ (e.g. DP = 26 gives m/z 4528.91) and linear polymer series with benzyl alcohol end-group, $[P_L + Na]^+$ (e.g. DP = 24 gives m/z 4310.73). The less intense red series may be assigned to the sodium adduct of the linear polymer with the loss of 1 CO_2 .

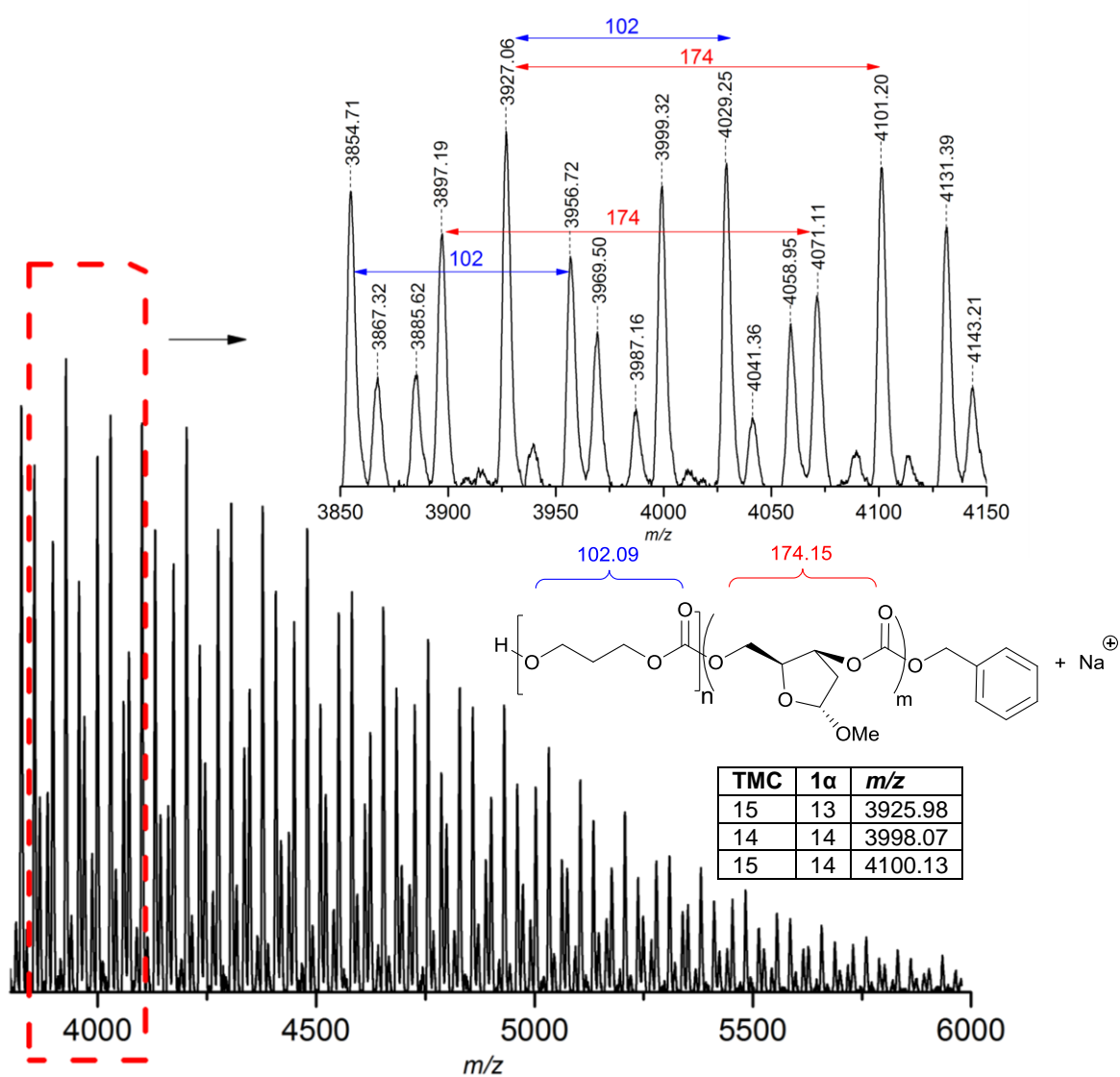


Fig. S30 MALDI-ToF MS of poly(TMC-co-47mol%-1 α) (Table 1, Entry 2), with benzyl alcohol and -OH end groups, flying as the sodium adduct.

8. TGA-MS

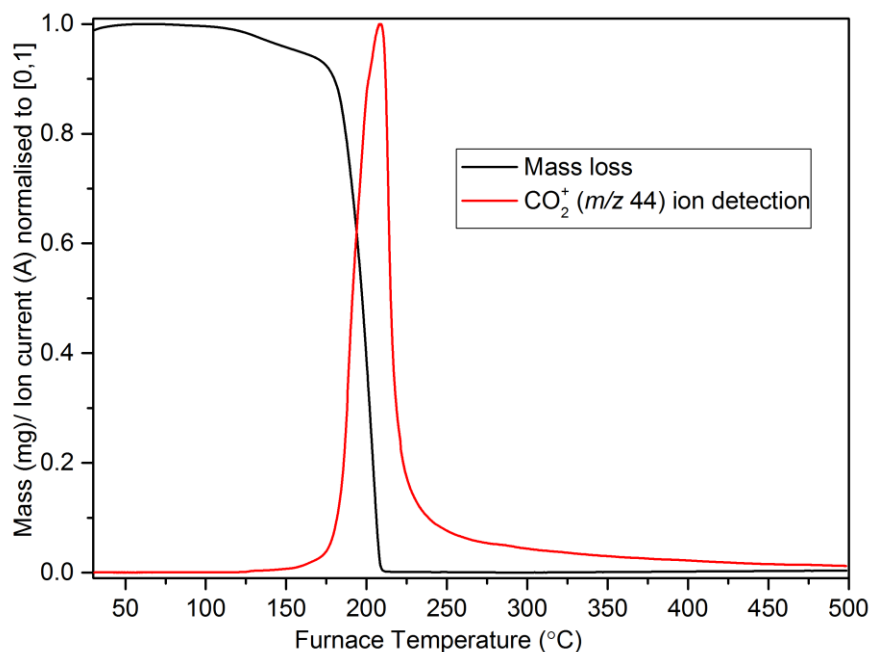


Fig. S31 TGA-MS of poly(TMC-co-66mol%-1 α). Plotted *versus* furnace temperature, the sample mass (mg) and m/z 44 ion current (A) are both normalised to [0,1] to aid plotting on the same graph.

9. Selected DSC Traces

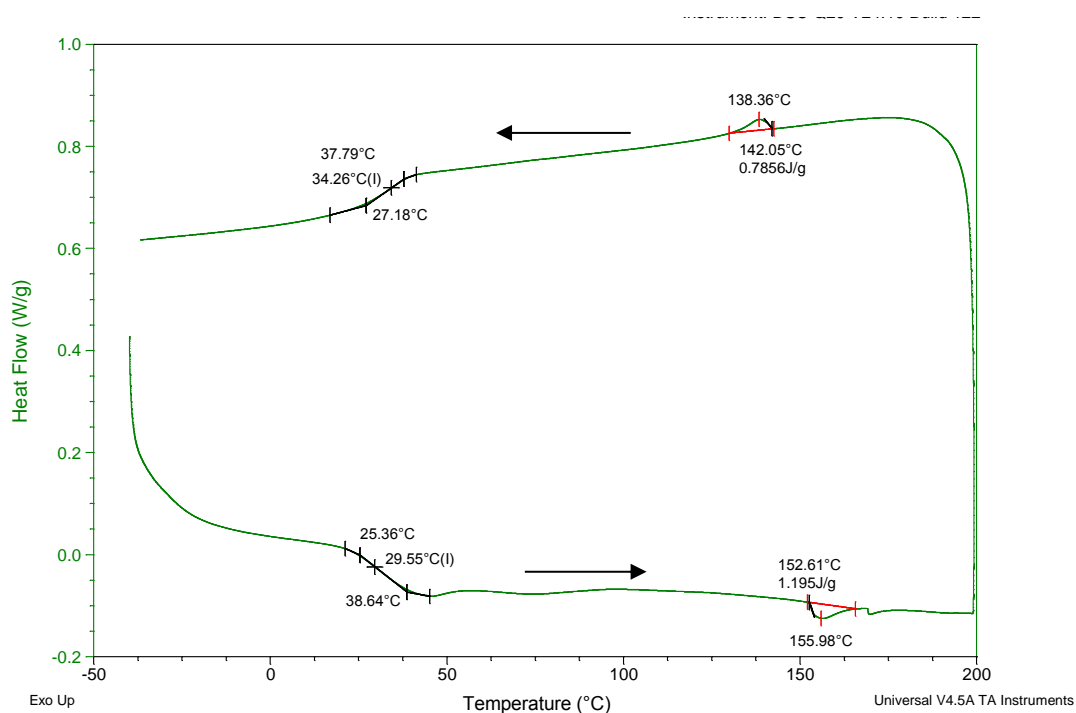


Fig. S32 First heating (-40 - 200 °C, 10 K min⁻¹) and cooling curve (200 - -40°C, 10 K min⁻¹) for poly(TMC-co-53mol%- α) (Table 3, Entry 5).

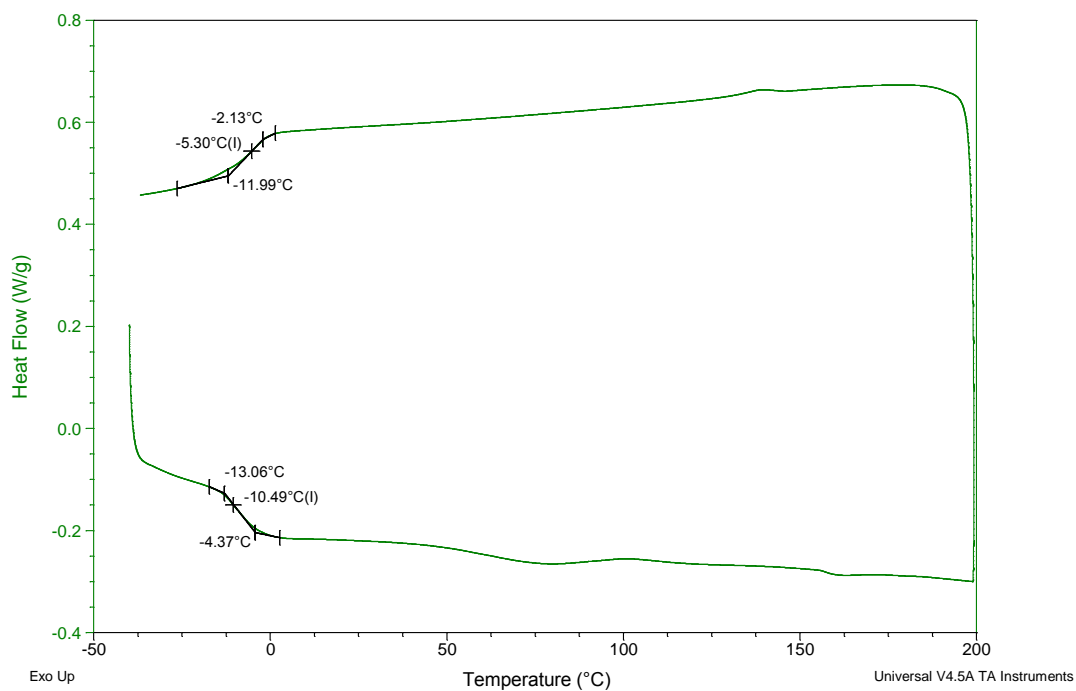


Fig. S33 First heating (-40 - 200 °C, 10 K min⁻¹) and cooling curve (200 - -40°C, 10 K min⁻¹) for poly(TMC-co-14mol%-α) (Table 3, Entry 9).

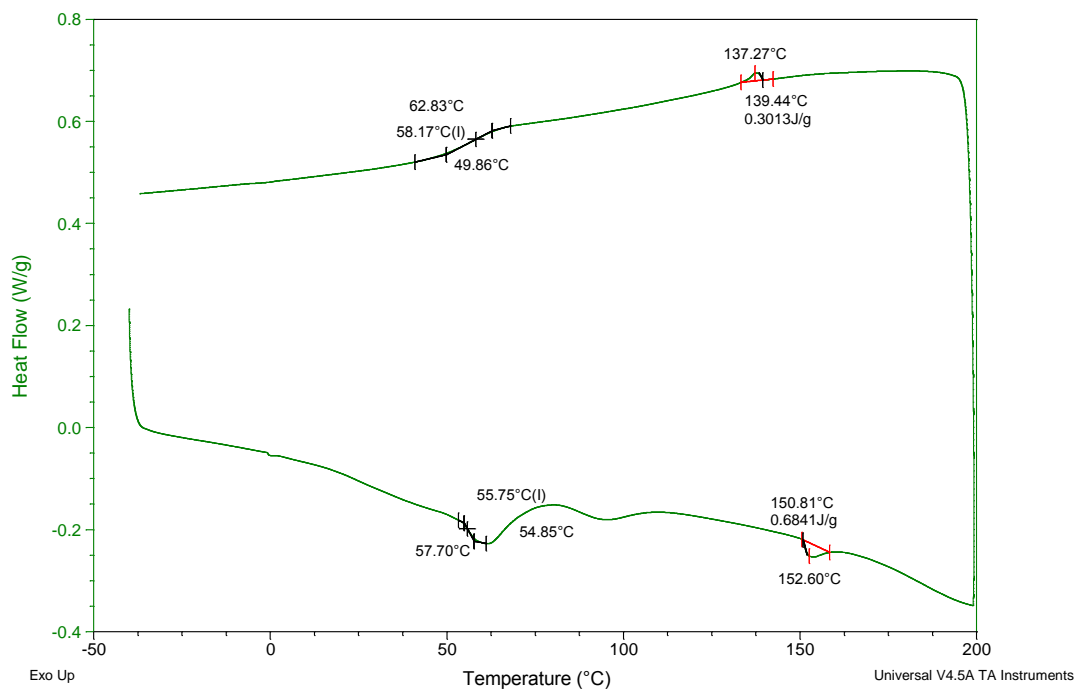


Fig. S34 First heating (-40 - 200 °C, 10 K min⁻¹) and cooling curve (200 - -40°C, 10 K min⁻¹) for poly(1α) (Table 3, Entry 1).

10. Powder Diffraction

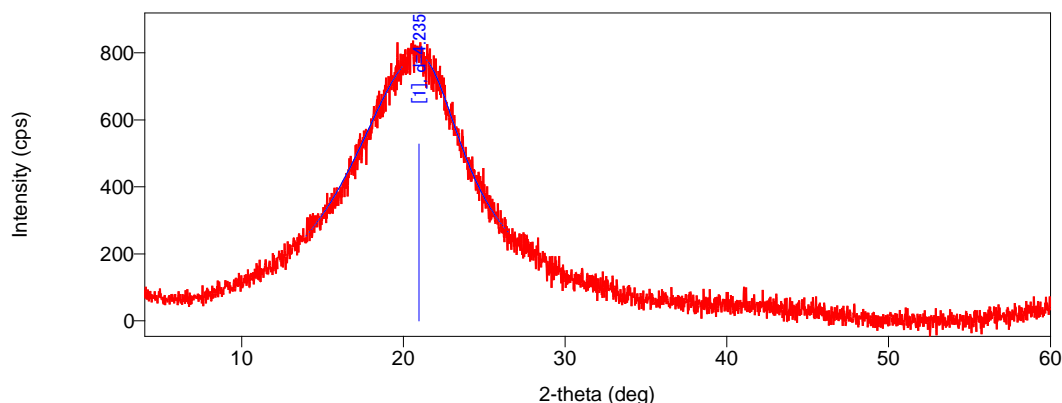


Fig. S35 Powder diffraction of selected copolymer, poly(TMC-co-66mol%-**1α**) showing amorphous nature.

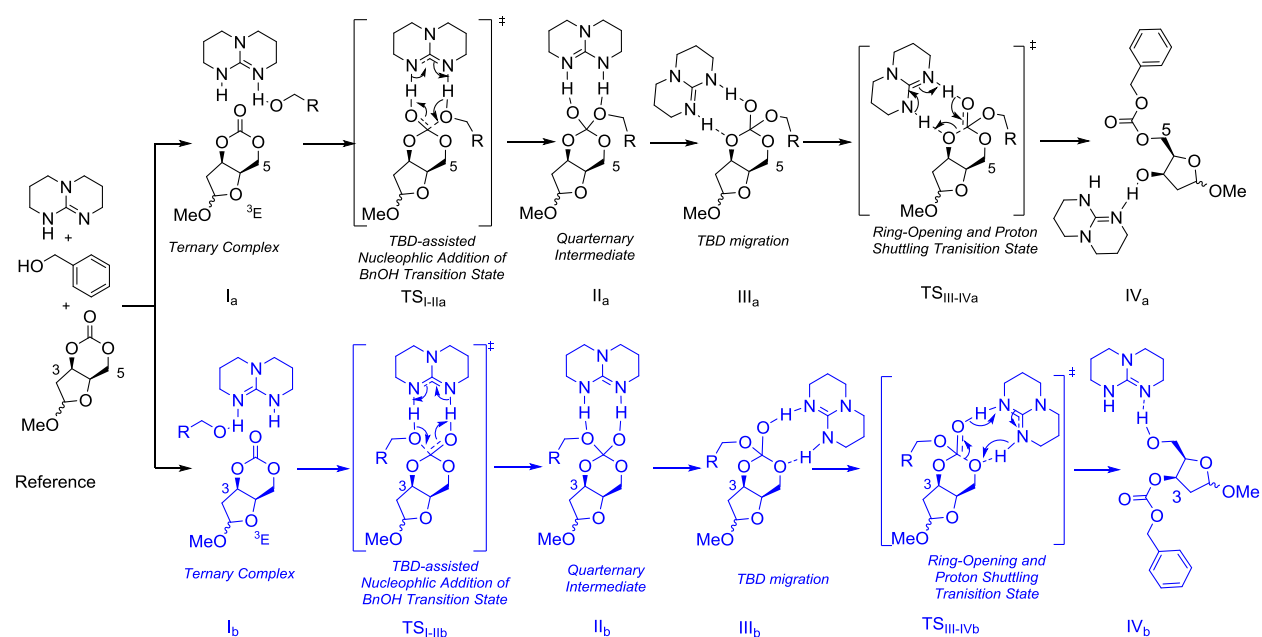
11. DFT Calculations

Geometries were fully optimised without any symmetry or geometry constraints, using the ω B97XD LC hybrid functional developed by Chai and Head-Gordon, which includes an empirical dispersion correction and has been shown to effectively reproduce thermodynamic and kinetic experimental data.¹⁻³ To confirm its nature, the vibrational data was used to relax the geometry of each located transition state (one imaginary frequency) toward reactants and products. No IRC calculations were performed to further confirm the identity. Only the most stable conformational isomers are reported for all intermediates.

11.1 Initiation Step in the ROP of **1α**, **1β** and TMC

For modelling of the ROP initiation step, a mixture of basis sets was selected; a higher basis set was used for key atoms (the carbonate, guanidine and alcohol moieties of **1**/TMC, TBD and BnOH) to account for potential anions and non-bonding (hydrogen bonding) interactions and a lower basis set for all other atoms to reduce the computational time. For steric reasons and after an initial Gibbs free energy screening, only attack of the benzyl alcohol at the face opposite to the β -OMe substituent was considered.

Full coordinates for all the stationary points, together with computed Gibbs free energy and vibrational frequency data, are available *via* the corresponding Gaussian 09 output files, stored in the digital repository: DOI: [10.6084/m9.figshare.4644574](https://doi.org/10.6084/m9.figshare.4644574).



Scheme S1 Typical scheme for the initiation step in the ROP of cyclic carbonates with TBD catalyst and BnOH initiator.

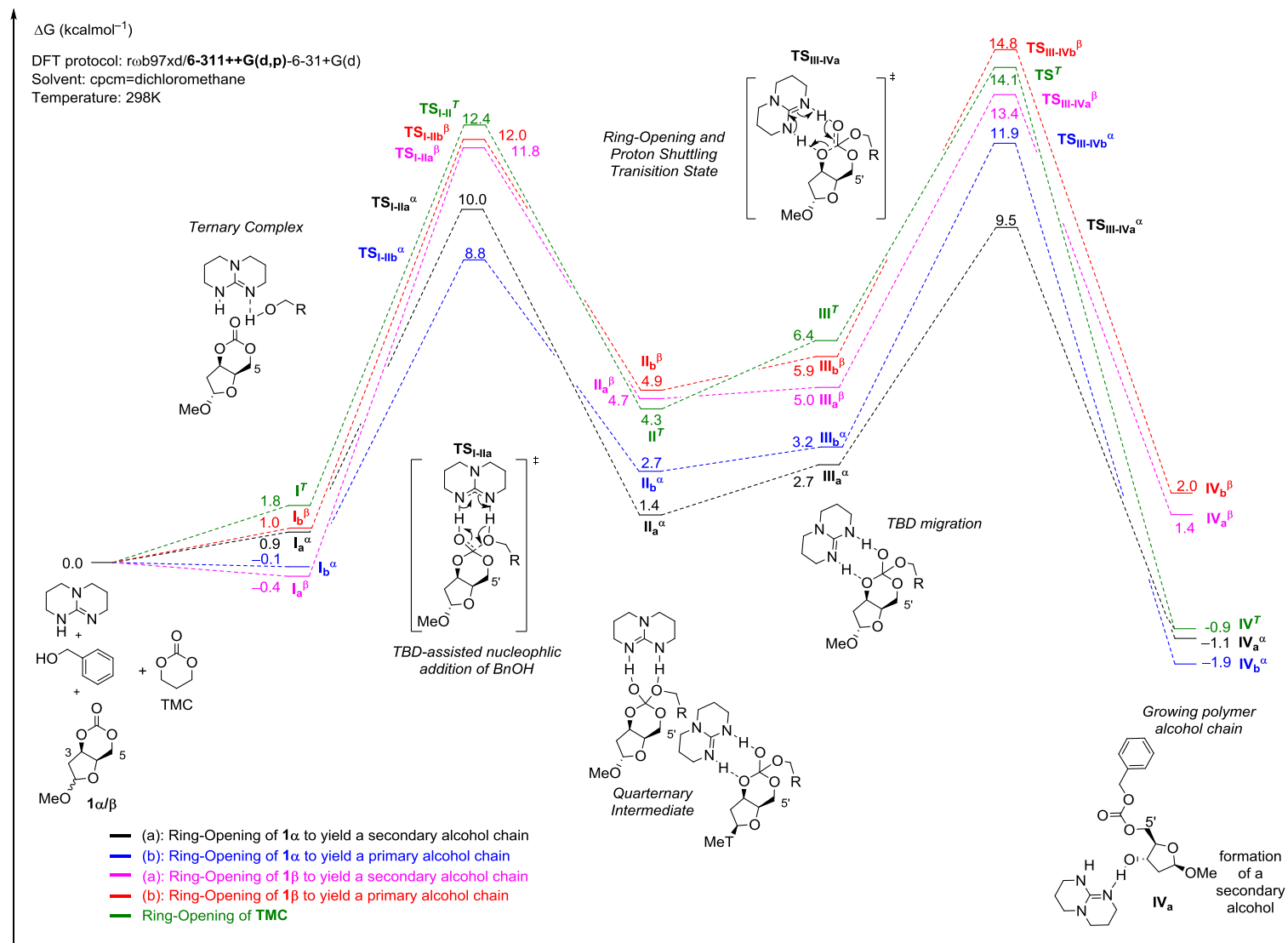


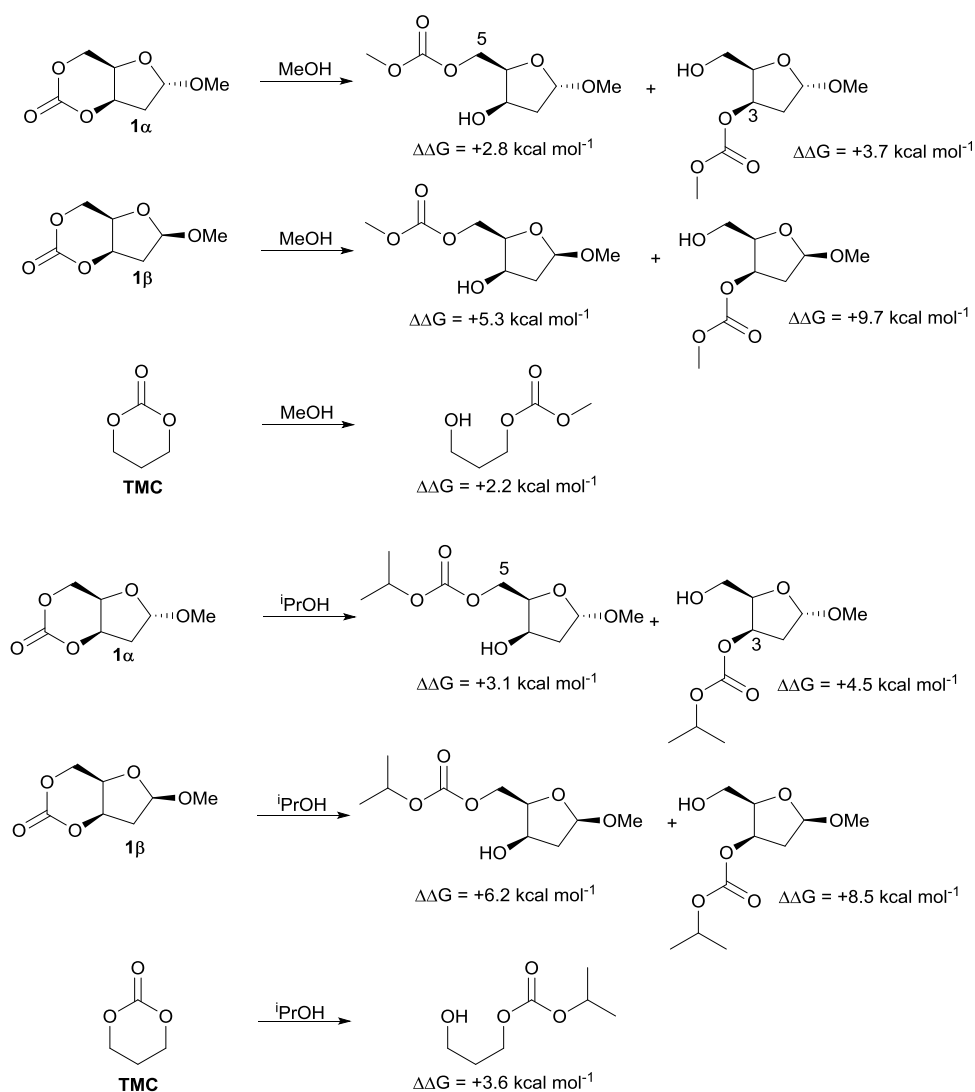
Fig. S36 DFT modelling of the initiation step in the ROP of 1α , 1β and TMC with TBD catalyst and BnOH initiator.

	Structure	G (Hartree)	ΔG (kcal mol⁻¹)
	1α	-648.498978	-
	1β	-648.502445	-
	TMC	-381.569395	-
	TBD	-438.513199	-
	BnOH	-346.523501	-
	1α + 1β + TMC + TBD + BnOH	-2463.607518	0 (reference)
Attack of 1α yielding a secondary alcohol chain	I_a^{α} (+TMC + 1β)	-2463.606158	0.9
	TS_{I-IIa}^{α} (+ TMC + 1β)	-2463.591526	10.0
	II_a^{α} (+ TMC + 1β)	-2463.605260	1.4
	III_a^{α} (+ TMC + 1β)	-2463.603273	2.7
	TS_{III-IVa}^{α} (+ TMC + 1β)	-2463.592375	9.5
	IV_a^{α} (+ TMC + 1β)	-2463.609247	-1.1
Attack of 1α primary alcohol chain	I_b^{α}	-2463.607652	-0.1
	TS_{I-IIb}^{α}	-2463.593471	8.8
	II_b^{α}	-2463.603172	2.7
	III_b^{α}	-2463.602453	3.2
	TS_{III-IVb}^{α}	-2463.588595	11.9
	IV_b^{α}	-2463.610514	-1.9
Attack of 1β yielding a secondary alcohol chain	I_a^{β} (+ TMC + 1α)	-2463.608178	-0.4
	TS_{I-IIa}^{β} (+ TMC + 1α)	-2463.588695	11.8
	II_a^{β} (+ TMC + 1α)	-2463.600032	4.7
	III_a^{β} (+ TMC + 1α)	-2463.599580	5.0
	TS_{III-IVa}^{β} (+ TMC + 1α)	-2463.586121	13.4
	IV_a^{β} (+ TMC + 1α)	-2463.605322	1.4
Attack of 1β yielding a primary alcohol chain	I_b^{β} (+ TMC + 1α)	-2463.605912	1.0
	TS_{I-IIb}^{β} (+ TMC + 1α)	-2463.588325	12.0
	II_b^{β} (+ TMC + 1α)	-2463.599639	4.9
	III_b^{β} (+ TMC + 1α)	-2463.598167	5.9
	TS_{III-IVb}^{β} (+ TMC + 1α)	-2463.583984	14.8
	IV_a^{β} (+ TMC + 1α)	-2463.604258	2.0
Attack of symmetrical TMC	I^T (+ 1α + 1β)	-2463.604716	1.8
	TS_{I-II}^T (+ 1α + 1β)	-2463.587781	12.4
	II^T (+ 1α + 1β)	-2463.600632	4.3
	III^T (+ 1α + 1β)	-2463.597317	6.4
	TS_{III-IV}^T (+ 1α + 1β)	-2463.584977	14.1
	IV^T (+ 1α + 1β)	-2463.608944	-0.9

Table S1 Computed Gibbs Free Energies at the ω B97XD/6-311+g(d,p)/6-31+g(d)/cpcm=dichloromethane/298K level of theory for the ring-opening of **1 α** , **1 β** and **TMC** by benzyl alcohol with TBD.

11.2 Monomer Ring Strain

11.2.1 Thermodynamics of ring-opening with MeOH/PrOH



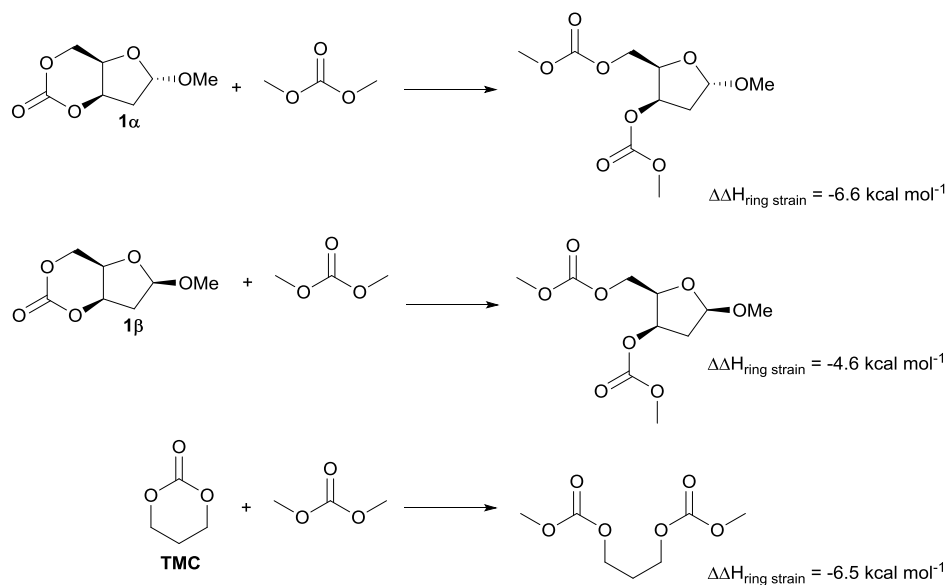
Scheme S2 Ring-Opening Thermodynamics ($\Delta\Delta G$) of **1 α** , **1 β** and TMC with MeOH and iPrOH at the $\text{rwB97XD/6-311+g(2d,p)/cpcm=dichloromethane/298K}$ level of theory.

Full coordinates for all the stationary points, together with computed Gibbs free energy and vibrational frequency data, are available *via* the corresponding Gaussian 09 output files, stored in the digital repository: DOI: [10.6084/m9.figshare.4644586](https://doi.org/10.6084/m9.figshare.4644586).

	Structure	G (Hartree)	$\Delta\Delta G$ (kcal mol⁻¹)
Starting Materials	Methanol	-115.702205	-
	iPrOH	-194.286844	-
	1α	-648.746770	-
	1β	-648.747521	-
	TMC	-381.648642	-
1α Products	MeOH + 1α	-764.448975	0.0 (reference)
	Ring-opening to 1° alcohol	-764.443008	3.7
	Ring-opening to 2° alcohol	-764.444442	2.8
	iPrOH + 1α	-843.033614	0.0 (reference)
	Ring-opening to 1° alcohol	-843.026393	4.5
	Ring-opening to 2° alcohol	-843.028605	3.1
1β Products	MeOH + 1β	-764.449726	0.0 (reference)
	Ring-opening to 1° alcohol	-764.434326	9.7
	Ring-opening to 2° alcohol	-764.441263	5.3
	iPrOH + 1β	-843.034365	0.0 (reference)
	Ring-opening to 1° alcohol	-843.020818	8.5
	Ring-opening to 2° alcohol	-843.024458	6.2
TMC Products	MeOH + TMC	-497.350847	0.0 (reference)
	Symmetrical ring-opening	-497.347387	2.2
	iPrOH + TMC	-575.935486	0.0 (reference)
	Symmetrical ring-opening	-575.929747	3.6

Table S2 Computed Free Gibbs Energies at the $\text{rwB97XD/6-311+g(2d,p)/cpcm=dichloromethane/298K}$ level of theory.

11.2.2 Isodesmic reaction with dimethylcarbonate



Scheme S3 Consideration of the ring strain of **1 α** , **1 β** and **TMC** by calculation of the enthalpy of isodesmic ring-opening with dimethylcarbonate ($\Delta\Delta H_{\text{ring strain}}$).

Full coordinates for all the stationary points, together with computed Gibbs free energy and vibrational frequency data, are available *via* the corresponding Gaussian 09 output files, stored in the digital repository: DOI: [10.6084/m9.figshare.4644577](https://doi.org/10.6084/m9.figshare.4644577).

Structure	H (Hartree)	$\Delta\Delta H$ (kcal mol⁻¹)
Dimethyl carbonate (DMC)	-343.512814	-
1α	-648.698158	-
1β	-648.700746	-
TMC	-381.611588	-
<i>DMC</i> + 1α	-992.210972	0.0 (reference)
1α oligocarbonate	-992.221438	-6.6
<i>DMC</i> + 1β	-992.213560	0.0 (reference)
1β oligocarbonate	-992.220930	-4.6
<i>DMC</i> + TMC	-725.124402	0.0 (reference)
TMC oligocarbonate	-725.134702	-6.5

Table S3 Computed Gibbs Free Energies at the rwB97XD/6-311++g(2d,p)/cpcm=dichloromethane/298K level of theory for the isodesmic ring-opening with dimethyl carbonate (DMC) of **1 α** , **1 β** and TMC.

12. Single Crystal X-Ray Structures

1a

Empirical formula	C ₇ H ₁₀ O ₅
Formula weight	174.15
Temperature	150(2) K
Wavelength	1.54184 Å
Crystal system	Orthorhombic
Space group	P2 ₁ 2 ₁ 2 ₁
Unit cell dimensions	a = 5.85770(10) Å α = 90°. b = 11.00620(10) Å β = 90°. c = 11.88280(10) Å γ = 90°.
Volume	766.096(16) Å ³
Z	4
Density (calculated)	1.510 Mg/m ³
Absorption coefficient	1.126 mm ⁻¹
F(000)	368
Crystal size	0.250 x 0.180 x 0.100 mm ³
Theta range for data collection	5.479 to 72.513°.
Index ranges	-7 ≤ h ≤ 4, -13 ≤ k ≤ 13, -14 ≤ l ≤ 14
Reflections collected	8745
Independent reflections	1517 [R(int) = 0.0229]
Completeness to theta = 67.684°	100.0 %
Absorption correction	Semi-empirical from equivalents
Max. and min. transmission	1.00000 and 0.68919
Refinement method	Full-matrix least-squares on F ²
Data / restraints / parameters	1517 / 0 / 110
Goodness-of-fit on F ²	1.108
Final R indices [I > 2σ(I)]	R1 = 0.0238, wR2 = 0.0590
R indices (all data)	R1 = 0.0239, wR2 = 0.0590
Absolute structure parameter	-0.04(6)
Extinction coefficient	n/a
Largest diff. peak and hole	0.128 and -0.173 e.Å ⁻³

1β

Empirical formula	C ₇ H ₁₀ O ₅
Formula weight	174.15
Temperature	150(2) K
Wavelength	1.54184 Å
Crystal system	Orthorhombic
Space group	P2 ₁ 2 ₁ 2 ₁
Unit cell dimensions	a = 7.56590(10) Å α = 90°. b = 9.9805(2) Å β = 90°. c = 10.2418(2) Å γ = 90°.
Volume	773.37(2) Å ³
Z	4
Density (calculated)	1.496 Mg/m ³
Absorption coefficient	1.115 mm ⁻¹
F(000)	368
Crystal size	0.250 x 0.200 x 0.150 mm ³
Theta range for data collection	6.192 to 72.264°.
Index ranges	-9 ≤ h ≤ 8, -11 ≤ k ≤ 12, -12 ≤ l ≤ 12
Reflections collected	4290
Independent reflections	1497 [R(int) = 0.0225]
Completeness to theta = 67.684°	99.8 %
Absorption correction	Semi-empirical from equivalents
Max. and min. transmission	1.00000 and 0.69375
Refinement method	Full-matrix least-squares on F ²
Data / restraints / parameters	1497 / 0 / 111
Goodness-of-fit on F ²	1.061
Final R indices [I > 2σ(I)]	R1 = 0.0241, wR2 = 0.0616
R indices (all data)	R1 = 0.0244, wR2 = 0.0621
Absolute structure parameter	-0.09(7)
Extinction coefficient	0.027(2)
Largest diff. peak and hole	0.163 and -0.150 e.Å ⁻³

13. References

1. A. Buchard, F. Jutz, M. R. Kember, A. J. P. White, H. S. Rzepa and C. K. Williams, *Macromolecules*, 2012, 45, 6781-6795.
2. J.-D. Chai and M. Head-Gordon, *Phys. Chem. Chem. Phys.* , 2008, 10, 6615-6620.
3. J.-D. Chai and M. Head-Gordon, *J. Chem. Phys.*, 2008, 128, 084106.